

Bachelor Degree Thesis

Degree in Industrial Technology Engineering

Design of a compressed air vehicle powertrain

The SG9C concept

REPORT

Author: Pau Sabater Garcia
Director: Carlos Sierra Garriga
Summons: July 2022



Escola Tècnica Superior
d'Enginyeria Industrial de Barcelona



To the memory of my dad, who always encouraged me to pursue my crazy dreams and who I wish he could see this project.

Abstract

These papers are intended to find out if an urban compressed air vehicle would be possible, so it could reduce the air pollution of cities and metropolises.

To answer that has been designed a powertrain for an air powered vehicle. The main components of it and those which have required a deep study and analysis are the pneumatic engine and the compressed air tank. The engine selected for this project has been the 9 chamber Di Pietro engine, invented by Angelo Di Pietro. The air tank chosen has been a type IV CNG (Compressed Natural Gas) tank, which are already used in mobility applications.

By the means of mathematical function extrapolation, vehicle dynamics simulations and other calculus referring to thermodynamics and fluids mechanics, among others, it has been demonstrated that an urban compressed air powered by the Di Pietro engine is capable enough to be a useful tool for city mobility and thus for fighting climate change.

Summary

SUMMARY	5
1. GLOSSARY	11
2. PREFACE	13
2.1. Origin of the project.....	13
2.2. Motivation	14
2.3. Previous requirements.....	14
3. INTRODUCTION	15
3.1. Project objectives.....	15
3.2. Project scope	16
3.3. Definition of the problem.....	16
3.4. Background.....	17
3.5. User analysis	17
3.6. Legislation.....	18
3.6.1. Light quadricycles (L6e).....	20
3.6.1.1. Light quadri-mobile for passenger transport (L6e-BP)	20
3.6.2. Heavy quadricycles (L7e)	21
3.6.2.1. Heavy quadri-mobile (L7e-C).....	21
3.7. Temporal planification of the SG9C.....	21
3.7.1. Invention.....	21
3.7.2. Concept design.....	22
3.7.3. Prototype testing.....	23
3.7.4. Homologation	23
3.7.5. Manufacturing.....	23
3.7.6. Launch.....	23
4. MARKET RESEARCH	25
4.1. Compressed air market research	25
4.1.1. Motor Development International prototypes	25
4.1.2. Di Pietro engine powered concepts and prototypes.....	27
4.1.2.1. Concepts.....	28
4.1.2.2. Existing prototypes.....	29
4.2. Citroën Ami 2020: the reference.....	30
5. THE DI PIETRO ENGINE	33
5.1. General description.....	33
5.2. Evolution of the engine	33

5.3. Components	34
5.4. How it works	36
5.5. Technical specifications	39
5.5.1. Power	39
5.5.2. Torque	41
5.5.3. Air consumption	42
5.5.4. Technical specifications summary	43
5.5.5. Tax horsepower	44
5.6. Noise and vibration	45
5.7. The MDI engine versus the Di Pietro engine	45
5.7.1. The MDI engine	45
5.7.2. Comparison between MDI and Di Pietro engines	46
6. THE AIR TANKS	48
6.1. Previous considerations	48
6.1.1. Thermodynamic air model	48
6.2. Air tank types	49
6.2.1. Characteristics of the selected tank	51
6.3. Available energy	52
6.4. Tank refilling	53
6.4.1. Previous considerations	54
6.4.2. Gas station refilling	54
6.4.3. Plug charging with a provided air compressor	54
6.4.4. Required work and heat loss	54
6.5. Input Air Temperature effect on autonomy range	54
7. AUTONOMY RANGE	56
7.1. Previous considerations of the autonomy study	56
7.1.1. Constant speed driving	57
7.1.2. Urban cycle	57
7.1.3. Passive resistances	58
7.1.3.1. Aerodynamic friction losses	59
7.1.3.2. Rolling friction	60
7.1.3.3. Hill climbing force	61
7.2. Autonomy range without considering the engine	61
7.2.1. At constant speed	62
7.2.2. ECE-15 cycle	63
7.3. Autonomy range considering the engine air consumption	64
7.3.1. At constant speed	64
7.3.1.1. Effect of different transmission relations	66
7.3.2. ECE-15 cycle	67

8. THE SG9C	68
8.1. Powertrain scheme	68
8.2. Chassis and body	68
8.3. 3D model	69
8.4. Refilling process.....	70
8.5. SG9C technical specifications	71
8.5.1. Vehicle theoretical maximum speed	71
8.5.2. Pressure loss in the pneumatic tubes	73
9. ENVIRONMENTAL STUDY	76
9.1. Current situation	76
9.1.1. Existing alternative solutions.....	76
9.2. Advantages and disadvantages of compressed air	79
9.2.1. Advantages	79
9.2.1.1. Energy Stored on Invested	80
9.2.2. Disadvantages.....	81
9.3. Environmental impact of the SG9C	82
9.3.1. Emissions	82
9.3.2. The air tanks.....	82
9.3.3. The chassis and body.....	83
10. ECONOMIC STUDY	84
10.1. Economic comparative	84
10.1.1. Refilling costs	84
10.1.2. Overall cost.....	84
10.2. Project implementation budget	85
CONCLUSIONS	86
ACKNOWLEDGEMENTS	87
BIBLIOGRAPHY	88
Bibliographic references.....	88

Figures and tables index

Figures

Fig. 1: Scheme of the manufacturing of a vehicle specified for a Di Pietro engine powered vehicle.

Fig. 2: The AirPod 2.0.

Fig. 3: AirPod planned models. Left: standard. Middle: pick-up. Right: cargo.

Fig. 4: Ford T2 Model.

Fig. 5: The Agnell Unit.

Fig. 6: Kangaroo motorcycle concept.

Fig. 7: Air powered moped concept.

Fig. 8: Airgo Fig. 9: O2 Pursuit.

Fig. 10: Suzuki G100 air bike.

Fig. 11: Prototype vehicles constructed by Angelo Di Pietro.

Fig. 12: Engineair prototype engines development evolution.

Fig. 13: Detail of the Prototype No. 4.

Fig. 14: 6-chamber Di Pietro engine. Left: front view. Right: rear view.

Fig. 15: Left: front view of the engine. Right: rear view of the engine.

Fig. 16: Front view of the inner mechanism.

Fig. 17: Engine control system. 1) Air channels. 2) Air distributor. 3) Rear cover.

Fig. 18: Cross section of the engine bonnet. 1) Air channel. 2) Air channel inlet. 3) Insert. 4) Outlet channel.

Fig. 19: Left: top view of the air distributor. Right: bottom view of the air distributor.

Fig. 20: Cross section of the air distributor. 1) Inlet air directioner. 2) Shaft hole. 3) Outlet air directioner.

Fig. 21: Working cycle of the Di Pietro engine in 9 visual steps.

Fig. 22: Cross section view of the inlet air trajectory.

Fig. 23: Top view of the inlet air trajectory.

Fig. 24: Centre-left view of the outlet air trajectory.

Fig. 25: Cross section view of the outlet air trajectory.

Fig. 26: Air exhaust through the cylindrical piston and shaft.

Fig. 27: Power versus engine speed of the 6C engine, by Monash University.

Fig. 28: Power versus engine speed extrapolated graphic of the 9C engine for different inlet air pressures, own source.

Fig. 29: Torque versus engine speed of the 6C engine, by Monash University.

Fig. 30: Torque versus engine speed interpolated graphic of the 9C engine for different inlet air pressures, own source.

- Fig. 31: Air consumption versus engine speed of the 6C engine, by Monash University.
- Fig. 32: Air consumption versus engine speed interpolated graphic of the 9C engine for different inlet air pressures, own source.
- Fig. 33: MDI's Engine power and torque curves.
- Fig. 34: MDI's engine
- Fig. 35: Type I, II, III and IV tanks internal structure schematic.
- Fig. 36: Internal structure of a type IV tank.
- Fig. 37: Tank refilling process.
- Fig. 38: ECE-15 urban cycle.
- Fig. 39: Rolling resistance coefficient as a function of speed.
- Fig. 40: Required energy with and without regenerative braking in the ECE-15 cycle.
- Fig. 42: Autonomy range as a function of inlet air pressure.
- Fig. 43: Autonomy range curves for different transmission relations.
- Fig. 44: SG9C's powertrain scheme.
- Fig. 45: Internal structure of MDI's prototype Green'air.
- Fig. 46: SG9C 3D model.
- Fig. 47: Theoretical maximum vehicle speed on flat surface.
- Fig. 48: Maximum theoretical vehicle speed in function of the engine's power.
- Fig. 49: Annual cobalt production of the Democratic Republic of Congo.
- Fig. 50: Solar cars. Left: Aptera. Right: Lightyear One.
- Fig. 51: Hydrogen fuel cell vehicles. Left: BMW iX5 Hydrogen. Right: Pininfarina H2 Speed.
- Fig. 52: ESOI for each type of energy storage technology.
- Fig. 53: Interest of compressed air vs electric cars from January of 2004 to June of 2022.

Tables

- Table 1: Gantt diagram of the future work needed to materialize the SG9C.
- Table 2: Technical specifications of the Citroën Ami.
- Table 3: Technical specifications of the Renault Twizy Urban 80.
- Table 4: Technical specifications of the Tazzari Zero City.
- Table 5: Technical specifications of the Di Pietro engine.
- Table 6: Comparison between the MDI engine and the Di Pietro engine.
- Table 7: Air properties inside the one type IV tank.
- Table 8: Mass distribution of the vehicle.
- Table 9: Rolling resistance coefficients depending of the surface.
- Table 10: Autonomy range for different constant speeds without considering the air consumption of the engine.

Table 11: Autonomy range for the ECE-15 cycle without considering the air consumption of the engine.

Table 12: Working chamber simulated supply parameters.

Table 13: Refilling costs comparative.

Table 14: Itemized cost list of the project.

1. Glossary

Parameters

ρ	Density	M	Molar mass of air
ν	Kinematic viscosity of air	μ	Dynamic viscosity of air
P	Pressure	P_j	Pressure for state j
T	Temperature	T_j	Temperature for state j
V	Volume	V_j	Volume for state j
v	Specific volume	v_j	Specific volume for state j
u	Specific internal energy	u_j	Specific internal energy for state j
h	Specific enthalpy	h_j	Specific enthalpy for state j
s	Specific entropy	s_j	Specific entropy for state j
ex	Specific exergy	Ex	Exergy
R	Universal gas constant	m_e	Inlet air mass
m_i	Initial air mass in the tank	m_f	Final air mass in the tank
m_{air}	Air mass stored in the vehicle	$m_{unladen}$	Unladen mass of the vehicle
$m_{passengers}$	Passengers mass	m_{cargo}	Cargo mass
m_{veh}	Mass of the unladen vehicle plus the on-board stored air mass	m_{total}	Total mass of the vehicle
η	Efficiency	Z	Compressibility factor
Q	Volumetric flow	AC	Air consumption
v_{air}	Air speed inside a tube	AR	Autonomy Range
$AR_{theoretical}^*$	Theoretical autonomy range without considering the air consumption of the engine	AR_{real}^*	Real autonomy range without considering the air consumption of the engine
A_f	Frontal area	C_d	Aerodynamic drag coefficient
ω	Angular speed	t	Time
P_{in}	Inlet air pressure	V_{STL}	Volume expressed in STL
$\ln()$	Natural logarithm	E_t	Tractive energy
X	Distance	C	Energetic consumption
F_{losses}	Total loss force	F_t	Tractive force
F_w	Aerodynamic friction losses	F_r	Rolling friction
F_g	Hill climbing force	N	Normal force
v_{veh}	Vehicle speed	a	Acceleration
g	Gravity constant	α	Road slope
A	Tube area	D	Tube diameter

Abbreviations

EV	Electric Vehicle	CAV	Compressed Air Vehicle
FWD	Front Wheel Drive	RWD	Rear Wheel Drive
6C	6-Chamber	9C	9-Chamber
MDI	Moteur Development International	GHG	Greenhouse gas
CNG	Compressed Natural Gas	ESOI	Energy Stored on Invested
WMCT	World Motorcycle Test Cycle	CAES	Compressed Air Energy Storage
WLTP	World Harmonized Light-duty Vehicle Test Procedure	STL	Standard litre: litre occupied by a gas at normal conditions (pressure of 1 bar at a temperature of 0 °C)

Non-SI Units

HP	Mechanical Horsepower	1 HP = 745,69987 W
rpm	Revolutions per minute	1 rpm = 0,10472 rad/s
mph	Miles per hour	1 mph = 1,61 km/h = 0,44704 m/s
bar	Bar	1 bar = 100000 Pa
psi	Pound per square inch	1 psi = 6894,75729 Pa
cc	Cubic centimetres	1 cc = 1 cm ³ = 1·10 ⁻⁶ m ³
STL/min	Standard litre per minute	1 STL/min = 1 L/min (air at atmospheric pressure)

2. Preface

Nowadays the automotive paradigm is changing so fast, and the vast majority of the car companies are going towards the electrification of its vehicles, manufacturing each year more hybrids and above all electric cars while they produce less petrol cars than the year before. It seems that soon or later all car companies will sell electric vehicles, or even some other clean alternatives that are gaining popularity recently, as hydrogen fuel cell vehicles. The automotive industry is going in this direction because there is no cleaner alternative energy. Or is it?

Everyone seems to have forgotten about air. Yes, air. Air is clean, free, and it has not to be produced because it is everywhere. Air powered cars basically run because air is compressed to a tank to be stored in the vehicles, to afterwards make the engine work with this air.

The present study is all based on a revolutionary compressed air engine invented by the Italian engineer Angelo Di Pietro. He named his pneumatic motor as the “Di Pietro engine”. His invention is a compact, lightweight and highly efficient rotary engine powered by compressed air, so it exhausts breathable air. One single engine is capable of powering a 600 kg car, and it has virtually no friction and doesn't produce significant noise, according to Mr Di Pietro.

2.1. Origin of the project

The desire of the author to design a car comes from a very young age. But as he grew up, the author got concerned about the huge challenge humanity faces called climate change and the catastrophic consequences it is already provoking nowadays and will provoke in the future. As the years passed, his desire got transformed into designing a sustainable car to put his automotive passion at the service of humanity.

These circumstances led to this project. The origin of this particular project goes back to February 2022, when the author, guided by his project tutor, discovered compressed air cars and how they work. For this reason, the author investigated about compressed air engines until he discovered Mr Di Pietro's invention. And the question came instantly to the author's mind: could this engine be the solution to pollution?

These papers will try to find this out.

2.2. Motivation

As it has been outlined before, the motivation of the author comes from his passion for cars and the automotive industry and also from his concern about the future shaped by climate change. For the author, is shocking how a so important device for people's lives such as automobiles have been so harmful to the environment and also to people's health.

Ironically, in the 21st century humanity is moving around with vehicles that "run an inefficient powertrain that is basically just an endless and exceptionally wasteful series of controlled explosions", as Cory Spondent once illustrated in TopGear's magazine.

For so, to preserve not only people's health, but also the planet's health, the author has turned his attention to compressed air vehicles, to see if they are better than the inefficient and harmful fossil fuel vehicles and also better than the not-so-clean electric vehicles. This last issue will be discussed in a further chapter.

To sum up, the motivation of the author is to do his bit in the fight against climate change through his passion.

Hopefully, apart from being the author's Bachelor Degree Thesis, these papers will not be just an academic work, but a step of a bigger research and a contribution to a better future.

2.3. Previous requirements

In this study are involved many concepts from the industrial engineering field, which specifically the main ones come from the field of mechanics, thermodynamics, fluids mechanics, algebra, calculus, programming and knowledge of the use of CAD software.

3. Introduction

The aim of this project is to discover if compressed air urban quadricycles would be a solution to the atmospheric pollution issue and a tool to fighting climate change in large and crowded cities around the world.

For so, this project will try to find out if it is possible to design a compressed air powertrain for an urban vehicle which has competitive technical specifications comparable to other petrol or electric vehicles of its segment. If so, this compressed air vehicle could be a serious alternative for urban mobility to take into account.

The quadricycle with the designed powertrain is intended to be driven in cities, so it has no need to reach high speeds. In Spain for instance most streets in cities have a 30 km/h maximum speed limit. For this reason, the top speed of the vehicle should be around 50 km/h, more than that for an exclusively urban vehicle would be pointless. Another feature of the vehicle is that it has to be very affordable, as much as possible. These circumstances lead to think about a small affordable city vehicle, and to be more specific, a quadricycle.

Considering the vehicle legally as a quadricycle implies a significant cost reduction in the vehicle production process. As commented, quadricycles do not reach high speeds, and for so for this type of vehicles are not required the safety measures that standard cars have. This does not imply an increase of danger because in case of accident, this would occur inside the city, at low speeds. For this reason, all the safety equipment a standard car needs is not required in a quadricycle, which brings the commented cost reduction.

To sum up, in order to fulfill all the specified conditions seen above, the vehicle designed in these papers will be a compressed air quadricycle.

3.1. Project objectives

The main objective of this project is, as commented previously, to design an air powered quadricycle powertrain as well as making an exhaustive study of the powertrain itself and its viability.

The powertrain should be able to propel the vehicle with two passengers and some cargo, and it should have an autonomy range of at least 50 km. The quadricycle is thought to have an enclosed passenger compartment, so the vehicle could be used comfortably in non-favourable climatologic conditions and could have acoustic isolation from the exterior. The parameters of the vehicle studied in these papers will have to fulfill the existing regulations.

To easily refer to the vehicle powered by the powertrain designed in these papers, the vehicle will be named as the SG9C.

3.2. Project scope

As commented before, as this project is a Bachelor Degree Thesis, it has the scope of 5 months, from February 2022 to early July 2022. However, the author will try this project to not remain just as an academic work, instead he will try to continue the path which leads to the materialisation of the SG9C.

This project consists on studying the viability of propelling a 600 kg urban vehicle with a Di Pietro engine, which is the pneumatic motor invented by Angelo Di Pietro.

3.3. Definition of the problem

The growth of big cities over the years have pointed the necessity of their habitants to move from one place to another in little time. Due to the large distance to cover, walking or human powered vehicles such as bikes are not an option for many people. To this has to be added the not big enough public transport infrastructure, reason why most people have private vehicles, being the immense majority of them powered by petrol.

This has led to an unsustainable situation in which cities are highly polluted and their population's health is badly affected. In fact, the scope of the air pollution crisis is bigger than is commonly thought. The effects of this problems on people's health but also on the planet's health are so severe that is humanity's obligation to fight against it. And so tries to do the author of these papers.

To put the magnitude of air contamination in context, here are just few examples of how catastrophic is:

- Polluted air breathing is a significant risk factor for a large number of diseases, such as respiratory infections, chronic obstructive pulmonary diseases, stroke, heart diseases and lung cancer, among others.
- It is estimated that 9 out of 10 people breathe dirty air to some degree worldwide.
- Air pollution is one of the principal causes of death around the world. It has been appraised that 4,21 million deaths are caused annually by just outdoor air pollution.
- Air pollution is estimated to have an annual cost to the world economy of \$5 trillion approximately due to the degraded quality of life and the productivity losses caused by the contaminated air breathing.
- Air dirtiness is responsible of atmospheric and climatologic changes such as the ozone depletion

or the acid rain.

In order to address the situation, this study pretends to see if compressed air vehicles are able to have an active role in the solution to pollution. And to do so, in these papers the author has tried to design a compressed air vehicle powertrain and energy storage system in order to see if compressed air cars can be the path to the sustainable mobility revolution.

3.4. Background

Before beginning with the compressed air powertrain itself, it would be interesting to see how the industry of automobiles has evolved and what can represent the compressed air vehicle in it.

The automotive industry has evolved and grown at a very fast pace over the years, and from the 2010s automobile manufacturers have destined more resources and research into electric cars, making them a pillar for the companies' future. The bet of these brands for EVs is so strong that some of them have promised they will not manufacture any internal combustion engine car in 2030, while others say the same but by 2040 or 2050. In addition, the hydrogen technology to propel cars is gaining support, as the necessity to reduce the carbon footprint.

But compressed air seems to be the forgotten technology for the automotive industry, specifically for urban mobility, and probably it is the best propulsion technology for this last application mentioned. Compressed air has so many advantages over the other propulsion technologies for land vehicles, which will be discussed in further chapters of the study. For so, this study is necessary to put the focus on compressed air, a technology little known by the vast majority of the population, and research about it. Compressed air technology applied for urban mobility can make a huge contribution in reducing the pollution of large cities to safe levels.

3.5. User analysis

The user analysis is a useful tool to know which people would interact or be affected directly or indirectly by the project. The most important users to consider are the main users and the operator users.

The main users are those for whom the project is intended and designed. They are the collective which will receive the benefits of the project. Otherwise, the operator users are those who perform operations on the device. In some cases, operator users may also be main users.

The users of a project can also be classified with the following criteria. Depending on their position in the system, users can be external, internal or third party. Depending on their relationship with the system, there may be voluntary or forced users. Finally, depending on how long they have been using

the system, they could be considered as regular users, sporadic users or accidental users, among others.

The main users of the vehicle which would be powered by the powertrain designed in these papers would be people that commute daily in their cities for any circumstances. Inside the main users' group can be found the following collectives:

Workers who go to work with a private vehicle

This group of people need a non-pollutant vehicle to be allowed to continue circulating, as environmental restrictions are getting stricter in most cities around the world. This type of user can also be considered as external, voluntary and regular users.

Teenagers between 16 and 18 years old

This collective needs a vehicle safer than a motorcycle that can be driven from the age of 16 years old in order to go to school or other places with more independence. The public transport is not an option for this group of teenagers, maybe because they live in isolated or rural areas with poor connection with public transport, and bikes are not an option either because the distances to cover are too long for them. This group can be considered as external, voluntary and regular users.

People without car license

This case is very similar to the previous one, with the difference that the users are adults and not teenagers. But as far as the user analysis is concerned about this group, they can be considered as main users, external, voluntary and regular users.

General citizens

This group needs and deserves to live in an environment free of smoke and pollution, or at least with less contamination than now. This collective is classified as third party, forced and regular users.

3.6. Legislation

As said in previous sections, the objective of these papers is to design the powertrain of a compressed air vehicle, which specifically is a quadricycle. And for so it is compulsory to know under which laws and normative will be regulated the vehicle.

Obviously, not all vehicles are regulated under the same laws. Each type of vehicle has its own normative and directives. To distinguish the different types of vehicles, the European Union elaborated a classification of them, which can be simplified for vehicles with 4 wheels or more in the following categories:

- Category L: light motor vehicles.
- Category M: vehicles destined to the transport of passengers and have at least four wheels.
- Category N: vehicles destined to the carriage of goods, also known as commercial vehicles.
- Category G: off-road vehicles.
- Category O: trailers (including semi-trailers).

Quadricycles are categorized in the category L, the light motor vehicles. Inside this group, there is another classification of all the existing light motor vehicles types, which is detailed in the following list.

L category:

- L1e: Light two-wheel powered vehicle.
 - L1e-A: Powered cycle.
 - L1e-B: Two-wheel moped.
- L2e: Three-wheel moped.
 - L2e-P: three-wheel moped designed for passenger transport
 - L2e-U: three-wheel moped designed for utility purposes
- L3e: Two-wheel motorcycle.
 - L3e-A1: low-performance motorcycle.
 - L3e-A1E: low-performance enduro motorcycle.
 - L3e-A1T: low-performance trial motorcycle.
 - L3e-A2: medium-performance motorcycle.
 - L3e-A2E: medium-performance enduro motorcycle.
 - L3e-A2T: medium-performance trial motorcycle.
 - L3e-A3: high-performance motorcycle.
 - L3e-A3E: high-performance enduro motorcycle.
 - L3e-A3T: high-performance trial motorcycle.
- L4e: Two-wheel Motorcycle with sidecar.
- L5e: Powered tricycle:
 - L5e-A: Passenger tricycle.
 - L5e-B: Commercial tricycle.
- L6e: Light quadricycle.
 - L6e-A: Light on-road quad.
 - L6e-B: Light quadri-mobile.
 - L6e-BU: light quadri-mobile for utility purposes.
 - L6e-BP: light quadri-mobile for passenger transport.
- L7e: Heavy quadricycle.

- L7e-A: Heavy on-road quad.
 - L7e-A1: A1 on-road quad.
 - L7e-A2: A2 on-road quad.
- L7e-B: heavy all terrain quad.
 - L7e-B1: all terrain quad.
 - L7e-B2: side-by-side buggy.
- L7e-C: Heavy quadri-mobile.
 - L7e-CU: heavy quadri-mobile for utility purposes.
 - L7e-CP: heavy quadri-mobile for passenger transport.

Depending on the characteristics of the quadricycle, it will be classified as a light quadricycle (L6e) or as a heavy quadricycle (L7e), because as the word “quadricycle” means, these are the only two categories for four-wheeled light motor vehicles. And to be more specific, the quadricycle of the present study can only be classified in one group inside each subcategory. In the case of light quadricycle (L6e) the suitable group for it would be the light mini car (L6e-B), while if the quadricycle designed in these papers is a heavy quadricycle (L7e), it would be specifically a heavy quadri-mobile (L7e-C).

In the following section is given a further explanation of the light and heavy quadricycles and their characteristics and legal restrictions.

3.6.1. Light quadricycles (L6e)

The Framework Directive 2002/24/EC defines light quadricycles as “four-wheeled motor vehicles whose unladen mass does not exceed 350 kg”. In the case of electric light quadricycles, the mass of the batteries is not included in this calculation. For so, if the analogy with the electric vehicle is made, for a non-existing-yet compressed air light quadricycle the air mass in the tank should not be included in the unladen mass as well.

The maximum speed of light quadricycles may not exceed 45 km/h, and in the case of those powered by spark ignition engines, their engine cylinder capacity cannot be more than 50 cm³. In the case of other internal combustion engines or electric motor, the net power output of these vehicles is not allowed to exceed 4 kW.

3.6.1.1. Light quadri-mobile for passenger transport (L6e-BP)

As seen, in the case the quadricycle designed would be in the L6e subcategory it would be also in the L6e-BP group, as the quadricycle of this study is intended to have an enclosed passenger compartment as regular cars have.

3.6.2. Heavy quadricycles (L7e)

The Framework Directive 2002/24/EC defines heavy quadricycles as “four wheeled vehicles (other than those referred to as light quadricycles) whose unladen mass does not exceed 400 kg if the vehicle is destined to the carriage of passengers or 550 kg if the vehicle is intended for carrying goods.” The mass of electric vehicles is not taken into account in this category as well, and neither should the mass of the filled air tanks. The design payload of heavy quadricycles cannot surpass 200 kg for passenger vehicles and 1000 kg for vehicles destined to the carriage of goods.

The net power output and maximum speed limits depend on the group inside the L7e subcategory.

3.6.2.1. Heavy quadri-mobile (L7e-C)

For the same reason as the light mini car (L6e-B), in the case the quadricycle of these papers is a heavy quadricycle, it can just fit in the heavy quadri-mobile (L7e-C) because of the enclosed passenger compartment.

The net power output of heavy quadri-mobiles is limited to 15 kW and the upper limit of their speed is 90 km/h.

3.7. Temporal planification of the SG9C

It would be undoubtedly good news if an urban vehicle based on the compressed air powertrain designed in these papers goes into production. But to manufacture a vehicle is not an easy process. Coming up next is described the temporal planification which takes the process of manufacturing the vehicle from its invention to the launch.

For car companies the entire process described below takes, on average, 72 months (6 years). To save time, manufacturers overlap the stages, as indicated in the process description.

3.7.1. Invention

The first step of the process is to plan which features and technical specifications are wanted the car to have. Here is where it is thought if it is wanted the future vehicle will be a family focused wagon, a powerful 4x4 all-terrain vehicle, a comfortable sedan, a fast sports car or, in this case, a zero-emission two-seater city focused agile small quadricycle powered by compressed air. The type of engine used and parameters such as curb weight, the maximum speed wanted or other performance goals are set in this part of the development process.

Apart from the aforementioned powertrain selection, in this step it is also done the market research and the customers are targeted, as well the users of the vehicle are identified. The initial considerations referred to budget, pricing or investment are also taken here. In some cases, in this phase of the process initial blueprint drawings are developed.

These papers are obviously part of this first step, which try to flatten the path to this vehicle to become a reality someday, hopefully sooner than later. However, they may not be this first step entirely, due to timing issue, as this present study has been developed for just 5 months, while car companies work on this stage for several month or even years.

Contrary to what is commonly thought, this stage comprehends from the first month to the 72th one, as in the continuous improvement methodology some of the parameters established in this phase may need to be redefined.

Licensing

This part is not a habitual step of the standard automobile production. In the case of these papers, in will be necessary this intermediate step before going to the concept design. This is because the engine used in this study, the Di Pietro engine, is patented by its inventor, Angelo Di Pietro. His company, Engineair Pty Ltd, has not the necessary resources to manufacture the Di Pietro engine, but is looking for other companies to become licensees and manufacture the engine. At this point, the Di Pietro engine could be used for manufacturing entire air powered vehicles, such as the one designed in these papers.

3.7.2. Concept design

In this second step are developed further blueprints and drawings of the vehicle, which will eventually be made using CAD (Computer Assisted Design) software, so there can be obtained representations of the designed vehicle with high precision.

For so, in this stage are sketched either the interior and the exterior. The materials required are chosen and aesthetic matters like colours and themes are designed.

Sometimes before going to the next step is necessary to go back to the invention stage, as while designing new considerations or approaches on parameters of the vehicle may arise. If this happens, it is desirable to happen in this step, as changes are cheaper to apply here than in further stages.

As the first step, the concept design phase also embraces the whole 6 years, for the same reasons explained in the previous step.

3.7.3. Prototype testing

In this third stage, it is built at least one fully functional concept vehicle, also known as prototype. The concept or concepts are evaluated through a huge variety of tests, which are intended to examine the vehicle's performance referred to speed, braking, handling, fuel-efficiency, emissions and safety.

This phase of the process takes from as soon as a fully functional prototype is built to the beginning of the manufacturing process. However, testing is carried out while the further stages of the process go on as well because of the continuous improvements that companies do.

3.7.4. Homologation

Depending on the results of the tests that have been carried out, the legal authorities grant the vehicle with the pertinent certifications. These legal certifications comprehend from fuel economy and emissions to safety aspects, among many other aspects.

In case that some results are not satisfactory, it is compulsory to return to the concept design stage, so the vehicle's parameters which have not obtained good results can be readjusted or even rethinking a new way to make the vehicle to succeed in where it has failed before.

The duration of this phase depends on the results of the testing, as they determine how many changes and improvements have to be applied.

3.7.5. Manufacturing

At this stage the vehicle is fully designed and where is materialized the final product.

The duration of this phase depends of the success of the vehicle. If it is successful and has demand over the years, the vehicle can be produced for many years, even decades. It starts when the vehicle has been given all the required certificates and homologations, and it ends when the brand decides to not sell anymore the vehicle, so it stops its production.

3.7.6. Launch

The final step is when the vehicle arrives to the public. The start of this step is often symbolized with spectacular presentations by the car makers in international motor shows, such as the International Geneva Motor Show or the Internationale Automobil-Ausstellung, also known as the Frankfurt Motor Show.

This step often is overlapped with the manufacturing process, as some brands allow to purchase a vehicle before it is built.

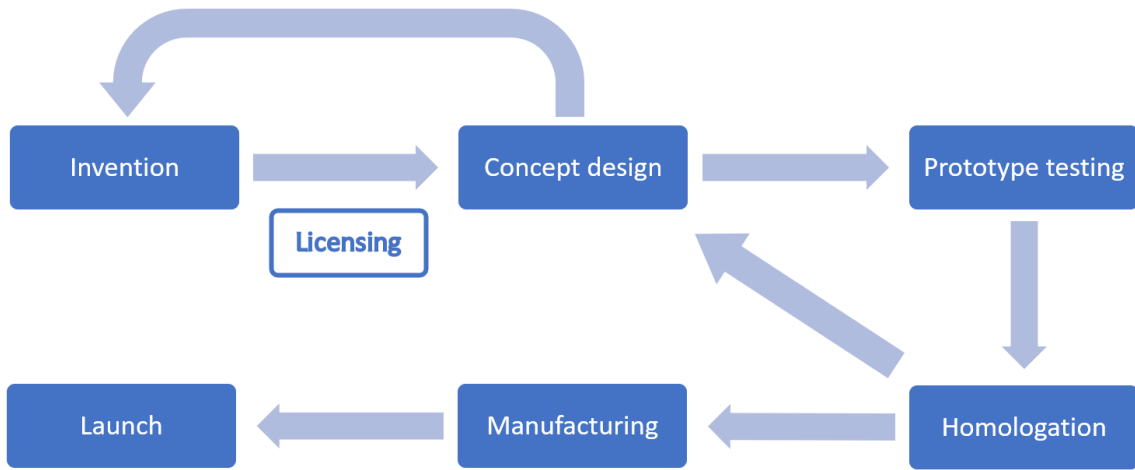


Fig. 1: Scheme of the manufacturing of a vehicle specified for a Di Pietro engine powered vehicle.

In the table 1 it is showed a Gantt diagram of the previously described process in case there was no need to do any redesign or continuous changes. The vertical line that separates the two halves of the first year indicates the ending of the present project. From July of the 1st year and on takes place the process of materialization of the SG9C described in this section.

	1st Year												2nd Year												3rd Year																
	January	February	March	April	May	June	July	August	September	October	November	December	January	February	March	April	May	June	July	August	September	October	November	December	January	February	March	April	May	June	July	August	September	October	November	December					
Invention	█																																								
Licensing							█																																		
Concept design													█																												
Prototype testing																									█																
Homologation																																									
Manufacturing																																									
Launch																																									

	4th Year												5th Year												6th Year															
	January	February	March	April	May	June	July	August	September	October	November	December	January	February	March	April	May	June	July	August	September	October	November	December	January	February	March	April	May	June	July	August	September	October	November	December				
Invention																																								
Licensing																																								
Concept design																																								
Prototype testing	█																																							
Homologation							█																																	
Manufacturing												█																												
Launch																																								

Table 1: Gantt diagram of the future work needed to materialize the SG9C.

4. Market research

Nowadays, in 2022 the market of compressed air vehicles is non-existent. Today there is not any purchasable vehicle powered by compressed air. For this reason, the air powered vehicle designed in this study will have to be compared to non-air powered vehicles.

It has to be said that some prototypes have been built and some of them patented during the last 30 years, despite that none of them have been materialised as a product for the public. Firstly, these compressed vehicles will be described briefly and afterwards will be analysed the market of heavy quadricycles, some powered by fossil fuels and others being electric.

4.1. Compressed air market research

In the following sections there will be presented all the theoretical concepts designed and all the functional prototypes built with the Di Pietro engine and with the MDI engine.

4.1.1. Motor Development International prototypes

The Motor Development International (MDI) society was created in 1991 by Guy Nègre, a former aircraft engine for tourism aviation and Formula 1 motor designer. Some compressed air prototypes have been developed at MDI since then.

But the MDI projects were years behind schedule. For instance, they planned to officially launch in Spain their final versions of their first prototypes during the second half of 2001, but never went into production.

Currently MDI keeps developing more prototypes, but any of them is expected to be manufactured and sold to the general public in the short term.

Although, MDI's engines are not totally eco-friendly. The engines developed by MDI can operate in two modes: in mono-energy mode, in which the engine runs exclusively on compressed air, and in dual energy mode, also called by MDI as its translation to French *bi-énergie*, mode which uses compressed air and petrol fuel.

The engine automatically uses the mono-energy mode while the vehicle is under 50 km/h. For speeds above 50 km/h, the motor uses the dual energy mode. Supposedly the fuel used in this second mode can be gasoline, diesel, biodiesel, natural gas, liquefied natural gas, ecological fuels, synthetic fuels or alcohol. MDI engine is a great improvement over the standard gasoline motors, but driving in the dual energy mode will have (although it can be small) a contribution to the environment pollution.

Fortunately, MDI has developed as well an engine that just runs on air (without the *bi-énergie* mode), and it is thought the newest prototypes and models are equipped with it.

MDI has built several prototypes and designed many more concepts, which can be consulted in the Annex B. Here will be seen their most important prototype, the AirPod 2.0.

The AirPod 2.0

The AirPod 2.0 is a heavy quadricycle (L7e category) developed by Moteur Developpment International, known as MDI. It is technically named the AirPod 2.0 because it is an evolution from the original AirPod.

The AirPod 2.0 is powered by a reversible compressed air motor with 430 cm³, 2 in-line cylinders each with active chamber, variable valve timing, aluminium crankcase and head. The engine offers a maximum power 10 HP at 1500 rpm and a maximum torque of 45 Nm from 250 to 1500 rpm.

The power is transmitted to the rear wheels through an electronically controlled gearbox with kinetic energy recovery during the deceleration phases. It has a three-speed gearbox (with the following ratios: 1st 2,54:1 - 2nd 1:1 - 3rd 0,4:1) and a reverse automatic gearbox. MDI claims the AirPod to reach a top speed of 80 km/h.

This vehicle is remarkably lightweight. Its chassis is made of fibreglass composite sandwich and polyurethane foam, and for so it only weights 350 kg. This weight is computed apparently with the air tanks empty. Moreover, the vehicle is 2,13 m in length, 1,5 m in width, has a height of 1,71 m and its wheelbase is 1,49 m long. It has two seats and 450 litres of room for cargo storage.

The AirPod 2.0 uses two tanks of 125 L each one, and the air is stored at a pressure of 248 bar (24,8 MPa). The tanks are made of thermoplastic coating with carbon fibre wiring, so they are classified as type IV tanks. This will be explained in more detail further in the study. With these characteristics, this vehicle is thought to have an autonomy range between 100 and 120 km, and capable to drive up to 150 km depending on how it is used.

A quirky feature of this vehicle is that it only has one single door, which is at the front, like the old BMW Isetta. But unlike the Isetta, the AirPod 2.0 front door opens upwards, like a butterfly door.

According to MDI licensee Air Mobility's webpage, the AirPod 2.0 is available from 11000 €.



Fig. 2: The AirPod 2.0.

The AirPod 2.0 can be manufactured with three different chassis: standard, pick-up and cargo. To reduce costs, all three versions are supported by the same base, so the different configurations are applied without the need to make significant changes in the manufacturing process. Below are showed the three different versions of the AirPod 2.0. However, the pick-up and cargo AirPods do not seem to go into production in the short term, as they do not even have an estimated price.



Fig. 3. AirPod planned models. Left: standard. Middle: pick-up. Right: cargo.

4.1.2. Di Pietro engine powered concepts and prototypes

Unlike the majority of MDI concepts, all the prototypes equipped with the Di Pietro engine have no harmful emissions, as it does not burn any type of fuel at any point. This makes the Di Pietro engine more environmentally friendly than the MDI motor.

As said before, there is not any compressed air vehicle in the market, so there is not any vehicle powered by the Di Pietro engine either. However, some theoretical concepts and functional physical prototypes have been built with the Di Pietro engine. These worldwide-made projects show the huge potential of this clean, efficient and affordable technology.

4.1.2.1. Concepts

Ford T² Model

This concept was designed by the Deakin University from Australia for the international contest launched by Ford to celebrate the century of existence of the Ford T Model. The contest consisted on designing the Ford T Model of the 21st Century. Deakin University won the first prize with this concept, a three-seater three-wheeler compressed air car powered with the Di Pietro engine. The pneumatic motor was aided by compressed natural gas for longer trips.



Fig. 4: Ford T² Model.

The Agnell Project

The Agnell Unit is an emergency motorbike designed by Marty Laurita for fire departments able to handle emergencies and non-emergencies. In emergency situations, this motorbike allows a faster response, as it can be stationed at firefighters' homes, decentralizing the fire department's lightweight vehicle fleet. In non-emergencies, where the immense majority of the calls are not life-threatening, this motorbike avoids sending a fire truck where in fact it is not needed.



Fig. 5: The Agnell Unit.

The Agnell Unit would have a top speed of 80 mph (129 km/h) and a range of 120 miles (193 km). Its estimated cost would be around \$7000.

Kangaroo motorcycle

The Kangaroo motorcycle was an industry-based project collaborating with the Car Design Research Network CDRN and Engineair. This motorbike has the Di Pietro engine attached directly to the rear wheel, so all the space a petrol engine could occupy is available for two compressed air bottles.



Fig. 6: Kangaroo motorcycle concept.

Air powered moped

This minimalist designed moped is powered by an Engineair motor fitted in the rear wheel, as the Kangaroo motorcycle does, so there is no need of chains or belts to transmit the power to the wheel. Behind the front wheel it can store three small bottles of compressed air.

The technical data of this moped, as well of the Kangaroo motorcycle, has not been provided. Although, it is suspected that both vehicles would have very competitive stats in their respective sectors due to their lightness and power supplied by their Di Pietro engines.



Fig. 7: Air powered moped concept.

Airgo

The Airgo is also a mobility object designed by Marty Laurita. It is a concept three-wheeler for light transport for people or cargo. With a range of 60 miles (96,56 km) and an estimated cost between \$500 and \$700, it is able to carry up to 800 lbs (362,874 kg) of weight.



Fig. 8: Airgo.

4.1.2.2. Existing prototypes

O₂ Pursuit

It is an air-powered dirt bike designed by Dean Benstead, which basically consist on a Yamaha WR250R frame with a scuba diving tank and a 9-chamber Di Pietro engine.

The original Yamaha WR250R has a curb weight of 132 kg, but the O₂ Pursuit weighs less as the petrol engine and many other components have been replaced by a lightweight compressed air powertrain. It is able to run 62 miles (99,78 km) before refilling the tank and can hit a top speed of 87 mph (140,013 km/h).



Fig. 9: O₂ Pursuit.

Suzuki G100 air bike

Students from Australia's Royal Melbourne Institute of Technology University, led by their professor Simon Curlis, reconverted an old petrol Suzuki G100 vintage racing bike into an air-powered bike with the Engineair motor. They said the motorbike is expected to surpass the 100 mph (160,934 km) barrier, and the engine to rev at 3000 rpm. The gear is fixed at a 1:1 ratio.



Fig. 10: Suzuki G100 air bike.

Angelo Di Pietro's prototypes

These are all the vehicles which Angelo Di Pietro has built with his engine and experimented over the last 18 years. These prototypes consist in a small sports car, a motorbike, as scooter, a forklift, a cargo and people three-wheeler carrier, a little truck, a go-kart and even a grass mower.



Fig. 11: Prototype vehicles constructed by Angelo Di Pietro.

Further in the study, once the Di Pietro engine is fully explained and the MDI motor is commented, both engines will be compared.

4.2. Citroën Ami 2020: the reference

In this study the car that is taken as a reference is the Citroën Ami 2020. This is a small city electric vehicle from Citroën which, in fact, is not a car, but a quadricycle.


The design of the Citroën Ami is focused in reducing costs, so it can be as affordable as possible. As a result, this quadricycle has double symmetry: the front and rear panels are interchangeable, and so are the doors. Because of this, the driver's door opens backwards (also known as suicide door) while the passenger door opens as standard.

As said before, this is not a car, it is a quadricycle, so it has not the obligation to reach the same safety standards as cars. For this reason, the Ami has no airbag or ABS. Moreover, to reduce costs the Ami also lacks of speakers, radio, electric windows, power steering or central locking among others. If these

shortcomings were in a standard automobile, it would be very unsafe. But as the vehicle is a quadricycle, it does not reach high speeds. Considering that is a vehicle for city mobility, in it the Ami's speed should not ever exceed 30 km/h inside city streets (which are limited to 30 km/h at least), although its top speed is 45 km/h.

Quadricycles can be driven without the need of a car license, just with a light motorcycle driving license. For this reason, quadricycles are an attractive mobility solution for teenagers, who do not have car licenses yet but need to gain freedom and independence. The exact age depends on the country. Additionally, quadricycles have some legal advantages respect "normal" cars. For instance, the normative for these vehicles is less strict than in cars' case, which make quadricycles way more affordable.

Following next are presented the technical specifications of the Citroën Ami.



Power	6 kW (8 HP)	Curb weight	485 kg
Torque	40 Nm	Length	2410 mm
Recharging time	3h	Width	1390 mm
Max speed	45 km/h	Height	1520 mm
0 - 45 km/h	10 s	Cd	0,4
Range	75 km	Frontal area	2 m ²
Category	L7e	Starting price (Spain)	7600 €

Table 2: Technical specifications of the Citroën Ami.


Although the Citroën Ami is the reference vehicle, there are other vehicles with similar characteristics that should be considered. In the tables below, are listed two more examples of comparable vehicles, so it can be seen a global picture of the market.

Renault Twizy Urban 80

The Renault Twizy is an urban electric quadricycle which began production in 2012 and still is. The version of the Renault Twizy comparable to the SG9C is the Renault Twizy Urban 80, because is legally classified as a heavy quadricycle (L7e).

It has a rear-wheel drive (RWD) transmission layout. The Renault Twizy Urban 80 has a 6,1 kWh lithium-ion battery which can be charged either with street electric charging facilities or with the 220 V and 10 A standard electric supply at home.

It has room for two people disposed in a tandem position, that is, the driver at the front and the passenger at the back. The Renault Twizy is noted to not incorporate doors as standard equipment, but as an option, which has to be paid more.




Power	13 kW (17 HP)	Curb weight	450 kg
Torque	57 Nm	Length	2338 mm
Recharging time	3,5 h	Width	1234 mm
Max speed	80 km/h	Height	1454 mm
Range	90 km (WLTP)	Starting price (Spain)	12985 €

Table 3: Technical specifications of the Renault Twizy Urban 80.

Tazzari Zero City

The Tazzari Zero City is an electric heavy quadricycle produced from 2009 until nowadays. Its engine is a 15 kW three-phase asynchronous motor. The Tazzari Zero City has a front-wheel drive transmission layout. Unlike the Renault Twizy Urban 80, it has two seats standardly arranged, that is, the passenger next to the driver, and it offers an enclosed passenger compartment as standard equipment.



Power	15 kW (20,12 HP)	Curb weight	450 kg
Torque	150	Length	2795 mm
Recharging time	9 h	Width	1500 mm
Max speed	90 km/h	Height	1450 mm
Range	94 km (WMTC)	Starting price (Italy)	17490 €

Table 4: Technical specifications of the Tazzari Zero City.

5. The Di Pietro engine

5.1. General description

The Di Pietro engine is a compact, lightweight and very efficient pneumatic engine capable of powering a 600 kg car. It was invented by Angelo di Pietro, a former Mercedes-Benz Wankel engine researcher and founder and CEO of Engineair Pty Ltd since the year 2000. Over all these years, Mr Di Pietro has improved the engine from its early prototypes to the newest ones. The latest versions of it are the 6-chamber and the 9-chamber Di Pietro engine. The 6-chamber engine is a little bit more powerful than the 9-chamber engine, but less efficient as well. In this project it has been used the 9-chamber Di Pietro engine.

Just to show an example of its power and efficiency, the 9C engine can replace a 1.6 litre 4-cylinder 90 HP (67,113 kW) diesel engine. Many years ago, the engine was tested in a vehicle, which was able to reach between 50 and 60 km/h going uphill. That vehicle had a 16 km range with a little 100 litre air bottle, and it took few minutes to refill. At the moment, for 15 cents could be refilled enough air to cover 3,2 km. Or, what it is the same, it cost less than 5 cents for each kilometre. All this is due to its remarkable efficiency, which is claimed to be up to 94,5% according to some studies.

5.2. Evolution of the engine

To achieve the 9C motor, Mr Di Pietro had been developing prototypes which evolved over the years, being each prototype lighter and more powerful than the previous one. This tendency of continuous improvement can be appreciated in the figure 12, which is a qualitative diagram that gives an idea of the weight and power of the 5 early prototypes constructed before the development of the 9C engine.

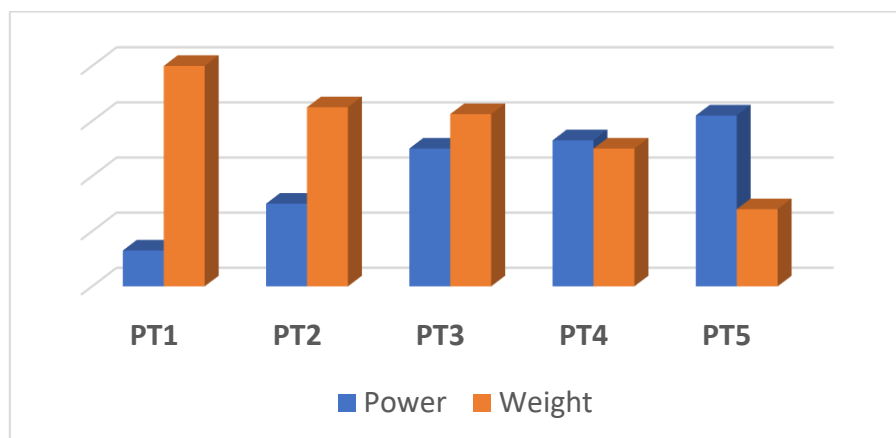


Fig. 12: Engineair prototype engines development evolution.

In the figure 13 it is detailed the prototype 4 (PT4, PT stands for “prototype”), which clearly has a similar aspect to the 9C engine, but very different in terms of its power-weight ratio.

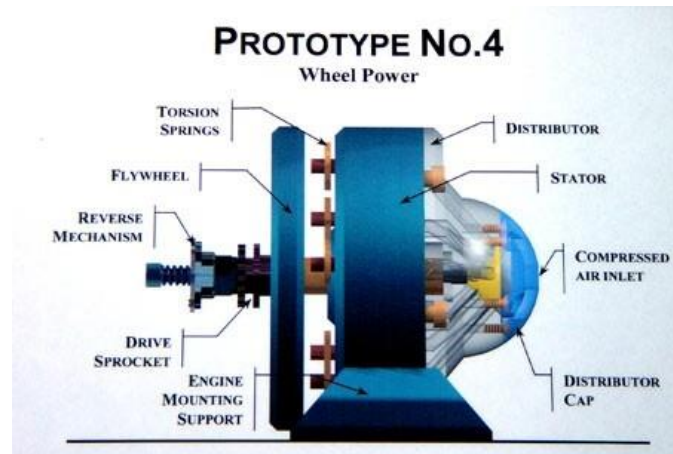


Fig. 13: Detail of the Prototype No. 4.

As commented, the most recent the engine is, the more powerful and lightweight is, and thus better power-weight ratio has, which can be appreciated in the figure 12. To be more exact, the 6-chamber motor, which is also the prototype 5 (PT5), is the penultimate engine that Angelo Di Pietro has constructed and the 9-chamber is the latest one. In the figure 14 is shown the 6C engine. The 9C motor is fully explained and detailed in the next section because, as it has been said, it is the pneumatic engine used in this project.



Fig. 14: 6-chamber Di Pietro engine. Left: front view. Right: rear view.

5.3. Components

In the figure 15 it can be observed the 9-chamber Di Pietro engine. As it has been explained, this is the selected compressed air engine to power the vehicle these papers try to design. On the left it is shown the front view of the motor, in which is appreciated its output shaft at the motor's centre or its 9 spiral springs, one for each expansion chamber. The function of these springs is to assist in the rotary oscillatory movement of the piston. It is important to notice that each one of the 9 spiral springs has

enough force to ensure that the cams do not lose contact with the cylindrical piston at higher speeds.

On the right of the figure 15 is seen the rear view of Engineair's motor. The hole in the middle is where the input air tube is attached.

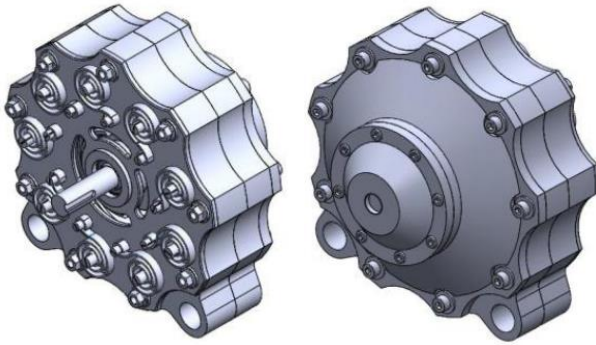


Fig. 15: Left: front view of the engine. Right: rear view of the engine.

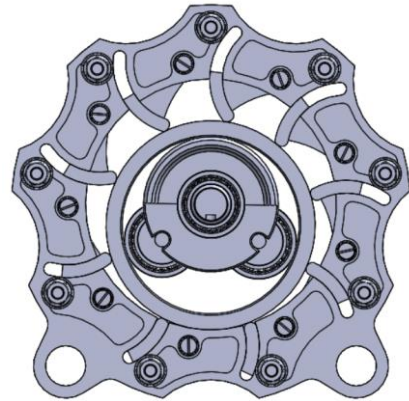


Fig. 16: Front view of the inner mechanism.

In the figure 16 the inner mechanism of the 9C Di Pietro engine is detailed. As it is shown, the rotary movement is transmitted by ball bearings. It is remarkable the few components used in this engine compared to standard motors.

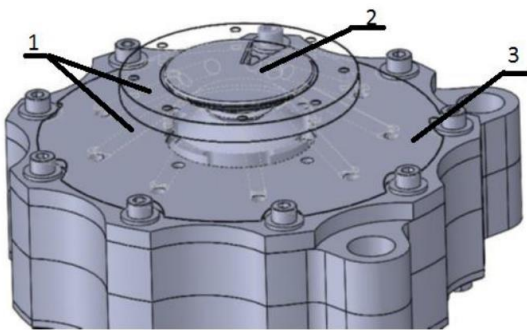


Fig. 17: Engine control system. 1) Air channels. 2) Air distributor. 3) Rear cover.

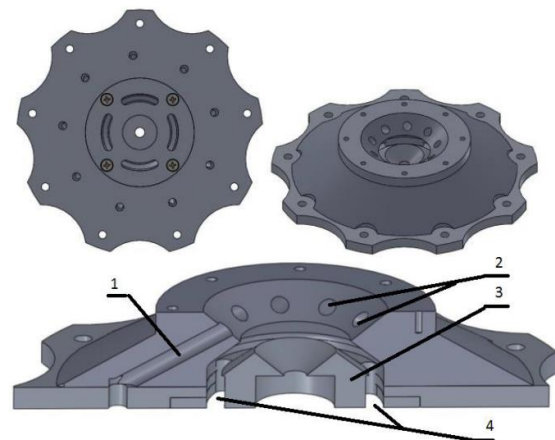


Fig. 18: Cross section of the engine bonnet. 1) Air channel. 2) Air channel inlet. 3) Insert. 4) Outlet channel.

The Di Pietro engine is designed in such a way that anytime just one chamber of the pneumatic motor is supplied, its two neighbouring chambers are closed and rest of them are directly connected to the atmosphere.

The engine's control system that ensures the motor to operate in this particular way is the air distributor. As it is shown in figure 19, the air distributor is a conic-shaped piece which has a smooth design in order

to minimize the energy losses. It is connected to the motor shaft, so it spins at the same speed as the shaft.

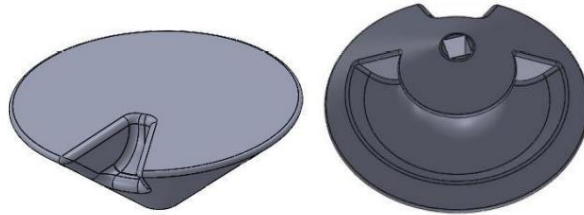


Fig. 19: Left: top view of the air distributor. Right: bottom view of the air distributor.

The air distributor directs the compressed air to the consecutive expansion chamber to be used while at the same time exhausts the air of the others chambers to the exterior by connecting them to the atmosphere.

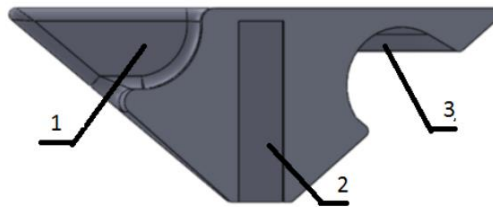


Fig. 20: Cross section of the air distributor. 1) Inlet air directioner. 2) Shaft hole. 3) Outlet air directioner.

The air distributor, as it can be suspected, it is collocated in the conical space slot right above the air channels entrance. It is remarkable to notice that this air distribution control is achieved without the need of any electronic circuitry.

5.4. How it works

The Di Pietro motor works as the following visual process shown on figure 21. Firstly, the inlet air is directed by the distributor (shown in yellow) through the inlet channel to the working chamber. Then, the air forces to move the cylindrical shaft eccentrically due to the air pressure on its outer wall. Finally, after the expansion of the air, it goes back to the air channel and through the distributor arrives to the outer channel, from which the air exhausts the engine.

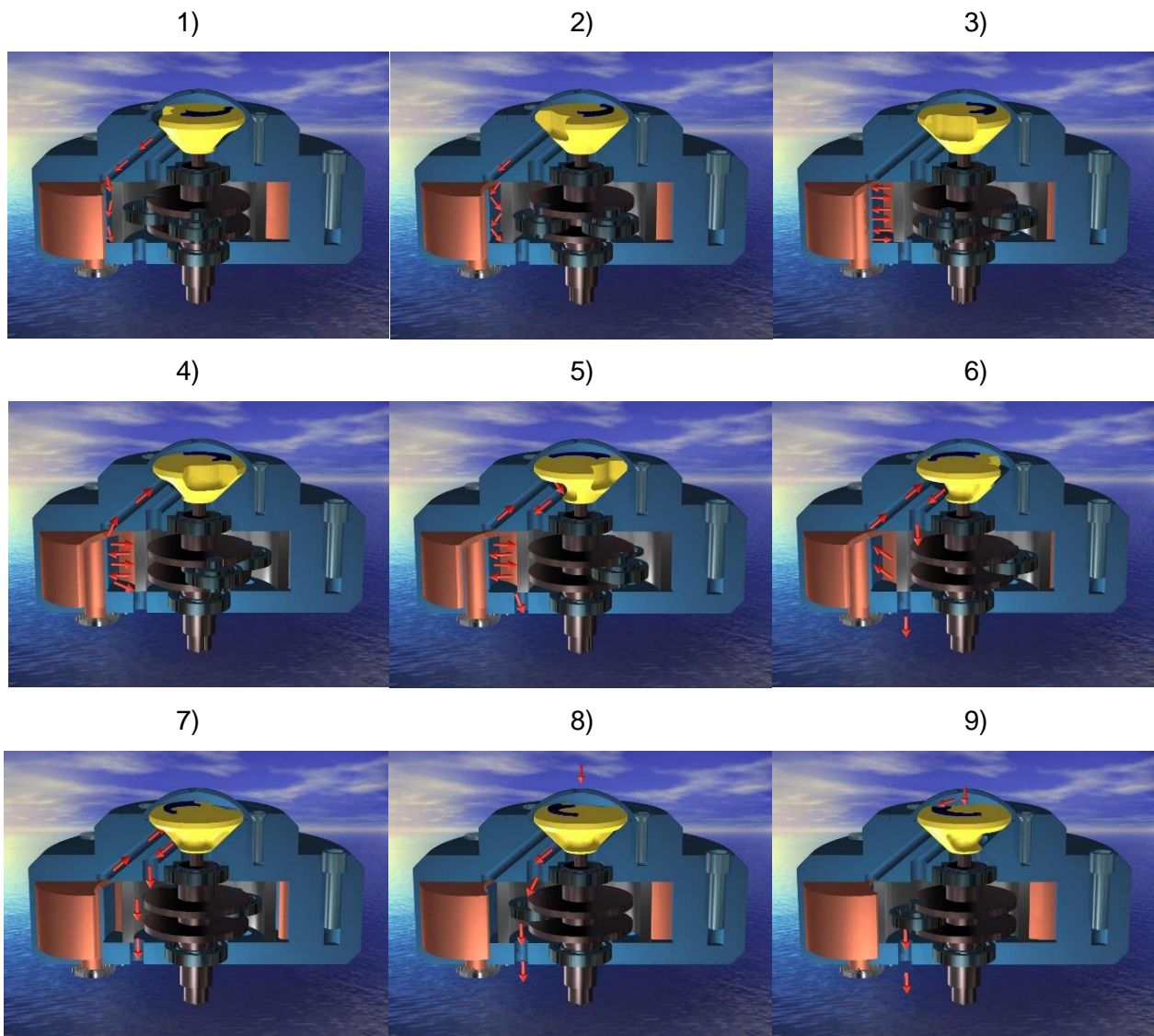


Fig. 21: Working cycle of the Di Pietro engine in 9 visual steps.

Just to visualize and clarify the engine's performance more, here is a 3D simulation made by Jaroslaw Zwierzchowski in which it can be understood how the air runs through the engine in different stages of the working cycle.

Firstly, in figure 22 can be appreciated how the compressed air enters the motor from the input air tube. Then the air is led by the inlet channel of the air distributor to one of the 9 air channels and gets to its correspondent expansion chamber. This same process can be seen in figure 23 from a different angle.

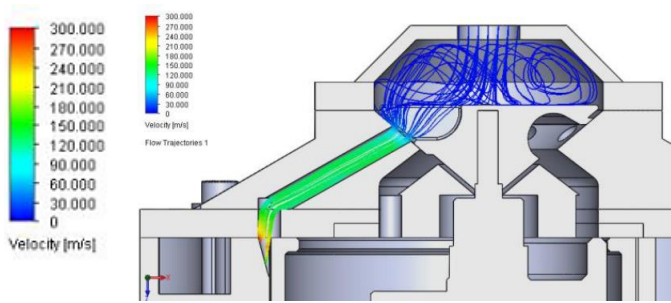


Fig. 22: Cross section view of the inlet air trajectory.

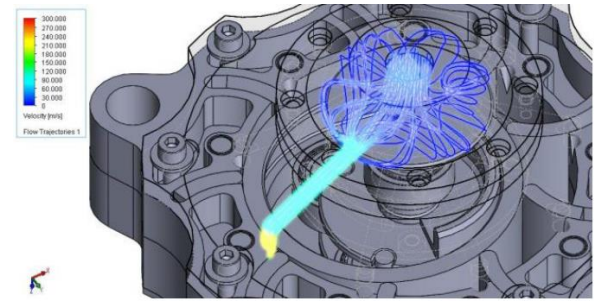


Fig. 23: Top view of the inlet air trajectory.

Once the air has expanded in the chamber and moved the cylindrical piston, it is compressed by the same piston and forced to return to the air channel. From it, the air goes through the outlet channel of the air distributor to the outlet channel of the engine's stator. This is shown on figures 24 and 25.

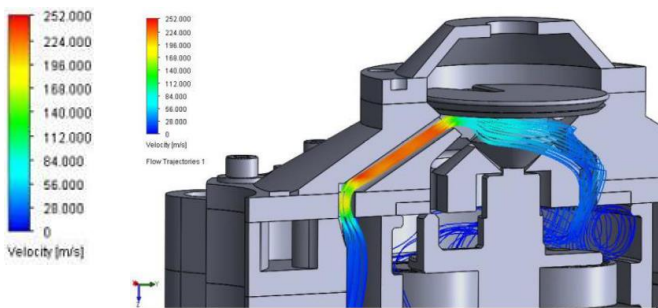


Fig. 24: Centre-left view of the outlet air trajectory.

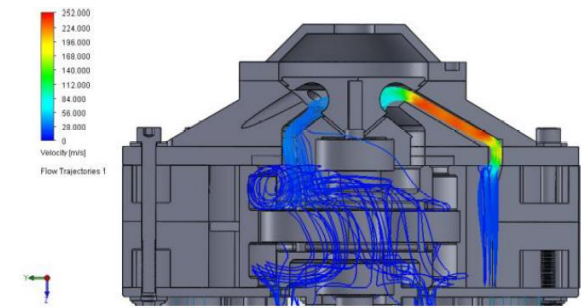


Fig. 25: Cross section view of the outlet air trajectory.

Finally, the air exits the outlet channel, passes through the cylindrical piston and the ball bearings and exhausts to the atmosphere. This final part of the process can be seen in the figure 26 below. Unlike internal combustion engines, the Di Pietro motor does not need a system to conduct and filter the outgoing gases, as it just consists of breathable air.

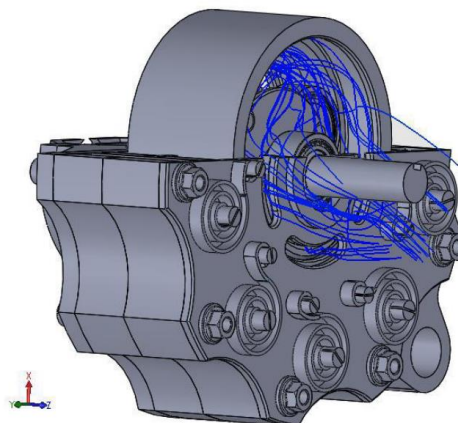


Fig. 26: Air exhaust through the cylindrical piston and shaft.

5.5. Technical specifications

Coming up next are represented the engine's operating diagrams that represent the power, the torque and the air consumption versus the rotary speed of the engine. Even though in this project is used the 9-chamber 399 cc Di Pietro engine, the following graphics are from the 6-Chamber 266 cc engine. This is caused by two main reasons. The first one is that these graphics were made back in 2007 by Monash University of Australia for their "Engine Performance Test Results", which they tested the 6C motor, not the 9C. Unfortunately, no testing or research has been published of the 9-chamber engine.

The second reason is that when the author contacted with Angelo Di Pietro himself to ask about first hand technical information of the 9C engine, the inventor kindly provided him with very useful data, in which among other things was one of those graphics constructed by Monash University.

Having seen that, the author assumed that although the 6C and 9C motor are not the same, both motors are similar, so the technical specifications of the 6C engine can give an idea about the performance and behaviour of the 9C motor.

Moreover, it has to be in mind that the 6-chamber motor is a bit more powerful but less efficient than the 9-chamber engine, so actually it must be expected a little less power and torque than it is shown on the charts but also fewer air consumption, which increases the range of the vehicle.

As it can be appreciated in Monash University's graphics, the 6C motor was just tested with two inlet pressures: 95 (6,55 bar, 655 kPa) psi and 136 psi (9,38 bar, 938 kPa). But as Mr Di Pietro indicated to the author, the inlet pressure can be up to 20 bar (2 MPa). Because of this, in order to determine an approximation of the curves for the full range of the inlet pressures, an own function interpolation has been carried out.

In the following section the 6C 266 cm³ Engine Performance Test Results by Monash University and the 9C 399 cm³ own extrapolated technical specifications are shown. The extrapolation procedure can be consulted in the Annex A.

5.5.1. Power

As it can be seen in the following graphics, there are two ways of scaling up the output power of the engine. The first one is to increase the inlet air pressure and the second way is to make the engine spin faster, increasing the air mass flow.

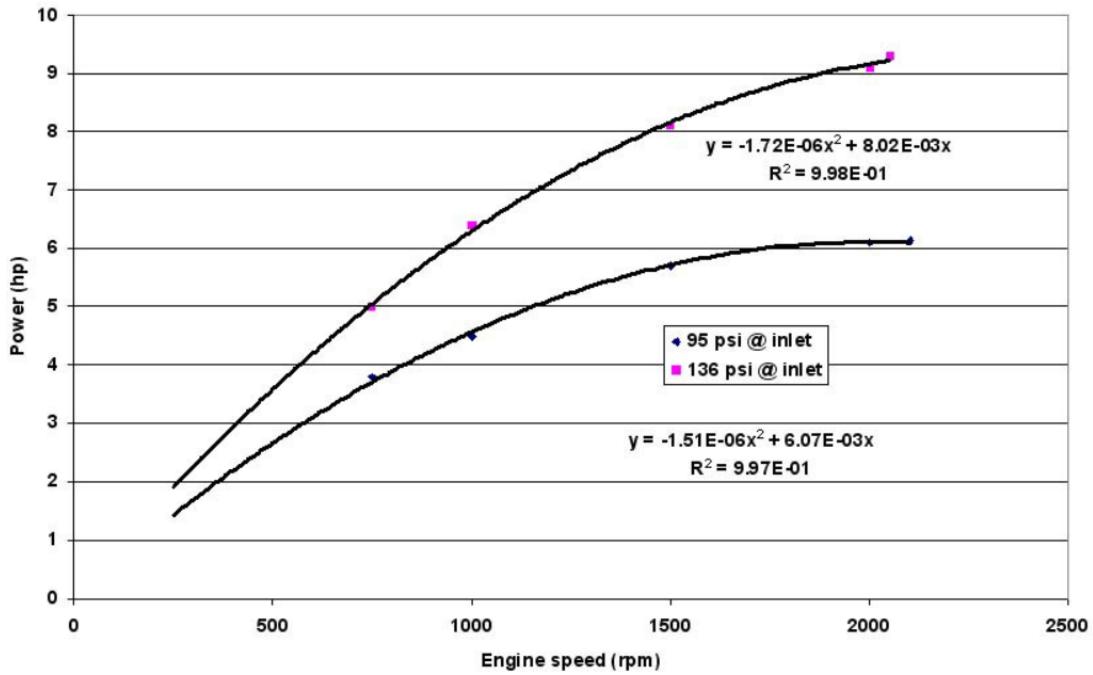


Fig. 27: Power versus engine speed of the 6C engine, by Monash University.

As it can be appreciated in the figure 28, the engine would have a maximum output power of 23 HP, which are 17,15 kW. However, this is an estimation and as it has been commented the real result may have little variation. Moreover, it has been considered that the engine is capable to rev at 2500 rpm at least, as Monash University’s graphic suggest.

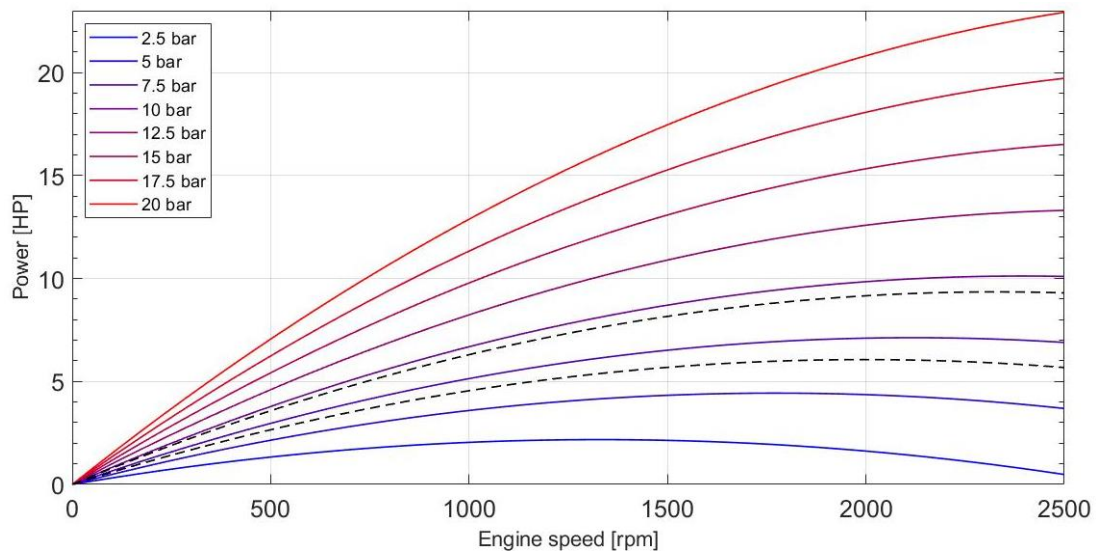


Fig. 28: Power versus engine speed extrapolated graphic of the 9C engine for different inlet air pressures, own source.

The dashed lines are the power curves drawn by Monash University, being the 95 psi (6,55 bar, 655 kPa) line the lower one and the 136 psi (9,38 bar, 938 kPa) the upper one. These two lines are the

reference from which the others have been interpolated. For this reason, the closer an interpolated line is to both reference lines, the more accurate they are. As a result, the further lines, such the one of 20 bar (2 MPa), might have more error, but to give an approximate idea it is more than enough.

5.5.2. Torque

Likewise, the power of the engine, the torque is also increased by increasing the inlet air pressure or increasing the engine speed.

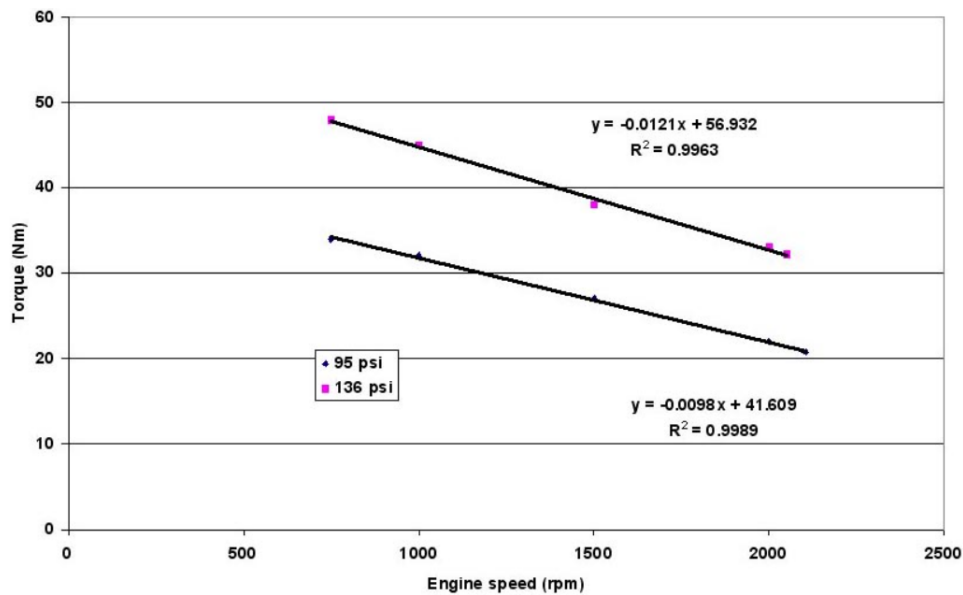


Fig. 29: Torque versus engine speed of the 6C engine, by Monash University.

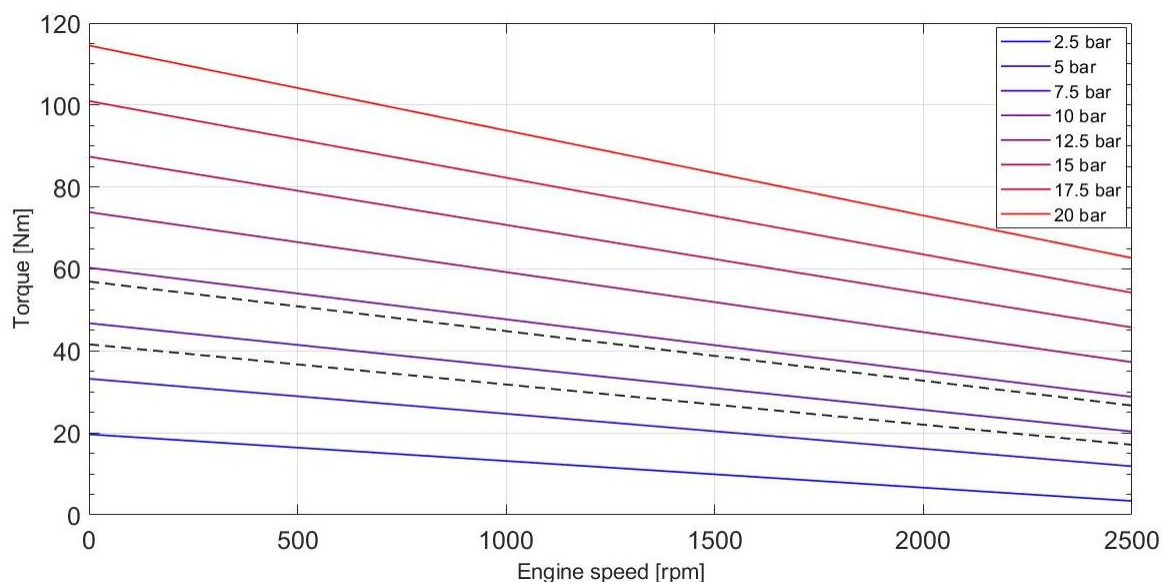


Fig. 30: Torque versus engine speed interpolated graphic of the 9C engine for different inlet air pressures, own source.

Assuming the validity of these extrapolations, the 9C Di Pietro motor is expected to offer nearly 115 Nm of maximum torque, as the figure 30 shows. The higher the inlet air pressure is, the more slope the lines have.

Once again, the two black dashed lines are the 95 psi (655,002 kPa, lower line) and 136 psi (937,687 kPa, upper line) curves of the 6C engine drawn by Monash University.

5.5.3. Air consumption

As it may be expected, the air consumption increases as the engine spins faster. Logically the autonomy range depends on the air consumption of the engine, which effects will be discussed and analysed in a further chapter.

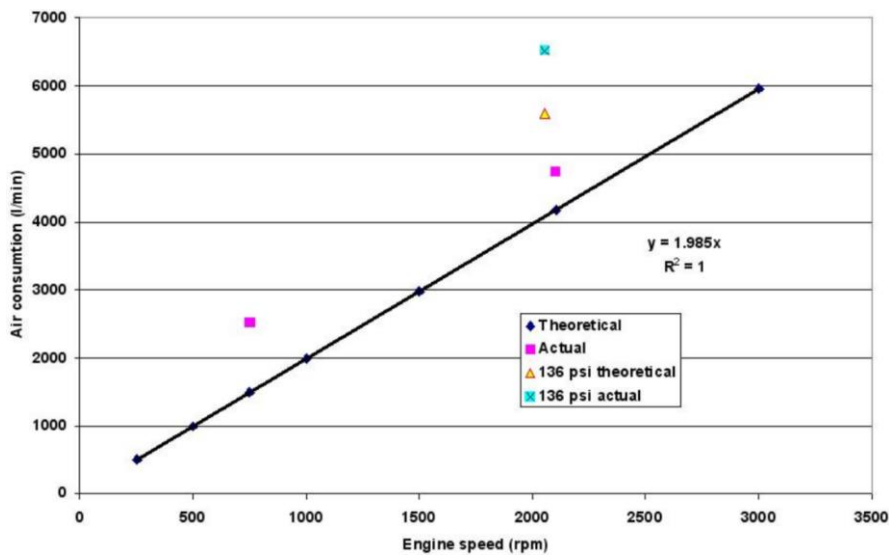


Fig. 31: Air consumption versus engine speed of the 6C engine, by Monash University.

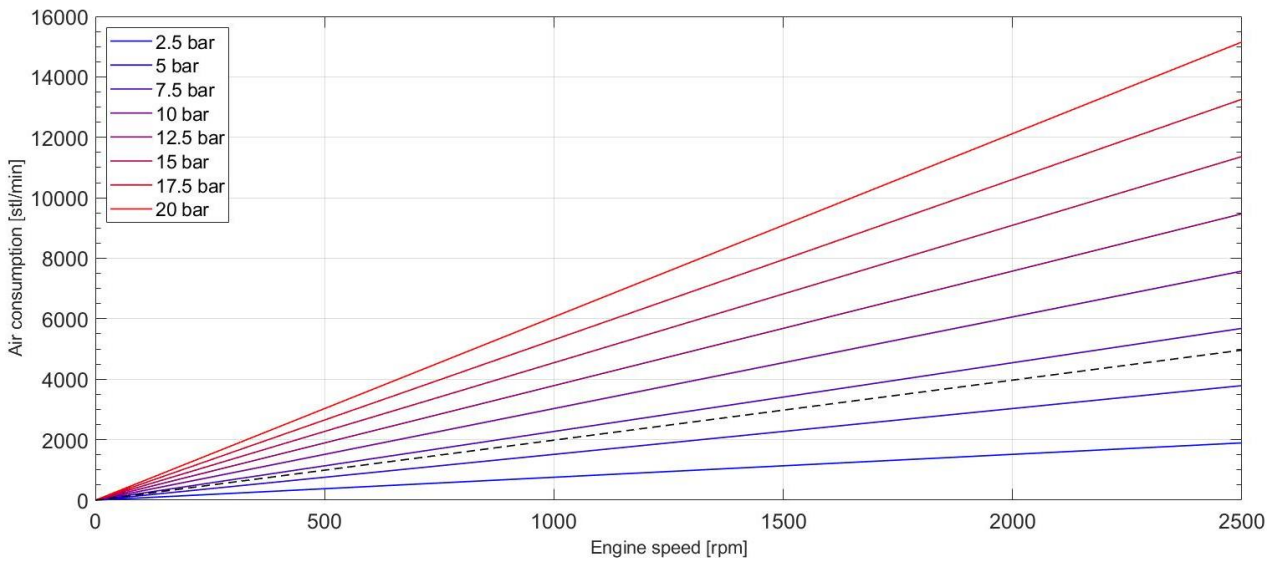


Fig. 32: Air consumption versus engine speed interpolated graphic of the 9C engine for different inlet air pressures, own source.

According to the figure 32, the maximum air consumption of the 9-Chamber Di Pietro engine would be 15152,6 STL/min, which equals to 19,26 kg/min of air. However, this is the case for an inlet air pressure of 20 bar, which is the maximum inlet air pressure indicated by Angelo Di Pietro to the author of this papers. Note that the higher the inlet air pressure is, the more slope the lines have. For lower pressures, the air consumption is lower as well.

5.5.4. Technical specifications summary

In this subsection are specified the most important technical specifications of the 9C Di Pietro engine.

N° of expansion chambers	9
Volume	399 cm ³
Weight	9,5 kg
Max. Power	17,15 kW (23 HP)
Max. Torque	115 Nm
Max. Engine Speed	2500 rpm (261,8 rad/s)
Max. Air Consumption	15152,6 STL/min = 19,26 kg/min
Minimum pressure to overcome friction	1 psi (6,9 kPa)

Table 5: Technical specifications of the Di Pietro engine.

Once the Di Pietro engine technical specifications are known, the whole vehicle parameters can be obtained. Having seen the capabilities of the engine, it seems clear that the quadricycle will be classified as a heavy quadri-mobile (L7e-C), inside the heavy quadricycle category (L7e).

There are many reasons to consider the SG9C a heavy quadri-mobile. To begin with, it is known that a single Di Pietro engine is capable to propel a 600 kg vehicle, which is more than the mass of the vehicle with two passengers and some cargo. Also, the Di Pietro engine is able to offer a net power output greater than the maximum power of L6e category vehicles, which is 4 kW (5,36 HP).

To fulfill the L7e-C regulation, theoretically the Di Pietro engine of the quadricycle would have to be limited so its maximum net power output is 15 kW, as it has been seen that it can offer up to 17,15 kW. However, it must be clear that due to the few information published of this topic and the assumptions the author has been obligated to consider, the real power output

may not exceed 15 kW, and for so may not be necessary the engine limitation.

In any case, it has been seen that the 9-chamber Di Pietro engine is able to offer enough power to propel an urban small vehicle.

5.5.5. Tax horsepower

The tax horsepower is a system which was created mainly for taxes purposes. Its value depends of the type of engine of the vehicle and, in the case of cylindrical piston engines, depends also on if it is a two or four-stroke engine, the number of cylinders and their dimensions. Following next are presented the formulas to calculate the tax horsepower used in Spain.

Cylindrical piston with straight displacement engines

This is the formula applied to the vast majority of petrol-powered vehicles.

$$P_f = T \cdot (0,785 \cdot D^2 \cdot R)^{0,6} \cdot N \quad (\text{Eq. 1})$$

Where in this equation P_f is the tax horsepower, T is 0,11 for two-stroke engines and 0,08 for four-stroke engines, D is the cylinder bore in centimetres, R is the stroke length in centimetres and N is the number of cylinders.

Electric motors and rotary engines

The electric vehicles and those which have a rotary engine, as the Wankel engine used mostly by Mazda, obtain their tax horsepower with the following formula.

$$P_f = \frac{P_e}{5,152} \quad (\text{Eq. 2})$$

Where P_f is the tax horsepower and P_e is the Effective or useful power of the engine.

The compressed-air vehicle designed in these papers will consider this last formula (Eq. 2), because the Di Pietro motor is a rotary engine, so it should be regulated under this category.

So, as seen in the section 3.6. about the legislation and knowing that the SG9C is a heavy quadricycle (L7e-C), the vehicle's maximum net power output will be at most of 15 kW, which are 20,12 HP. So, using the equation 2, it can be determined that the tax horsepower of the quadricycle designed will be at most of 3,904 HP (2,911 kW).

5.6. Noise and vibration

Two of the most remarkable features of the Engineair's motor are its virtual no friction and its little noise.

The motor does not vibrate at all, as it can clearly be seen at some of the recorded engine's performance demonstrations. This phenomenon is due to two main causes: the first one is that as this motor is a rotary engine, there are no unbalanced forces like those in petrol engines with cylinders. The second reason is that, as Mr Di Pietro points out, the motor consists of only 11 main components and most of them don't even touch each other because a thin film of air cushions the rotary motion of the piston.

As far as noise is concerned, the Di Pietro motor quietness is notable. Its noise levels are lower than any internal combustion engine, even when the pneumatic motor is revving at its maximum capacity. And there is no need to say that at low revolutions (per minute) it is almost silent. Furthermore, if it is wanted a higher level of quietness, it can be added an air muffler, turning the noise of the Di Pietro motor insignificant.

5.7. The MDI engine versus the Di Pietro engine

Having seen concepts and prototypes equipped with the Di Pietro engine and with the MDI engine, a comparison of both technologies can be carried out. But before the comparison, it is needed to explain the MDI engine, albeit briefly.

5.7.1. The MDI engine

In this subsection is explained the latest engine developed by MDI. As seen in the figure 34, it consists in an arranged in line 3 cylindrical piston engine which looks like a standard internal combustion engine. However, its pistons are not pushed by the expansion of the ignited fuel mix, they are pushed by timed bursts of compressed air.

In the figure 33 are presented the performance characteristics of the MDI's engine. According to MDI, it has a maximum power of 72 kW and a torque of 230 Nm. However, MDI says that if the engine is "boosted", it can achieve a maximum power of 90 kW and a torque of 285 Nm.

The engine revs at a maximum of 3000 rpm (314,16 rad/s) and weights 35 kg.

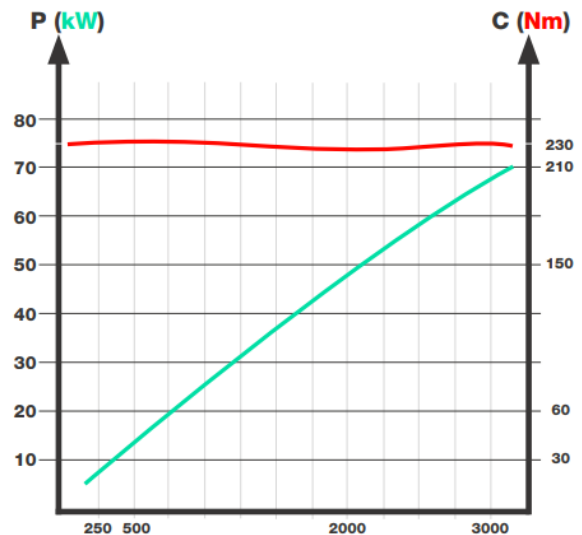


Fig. 33: MDI's Engine power and torque curves.

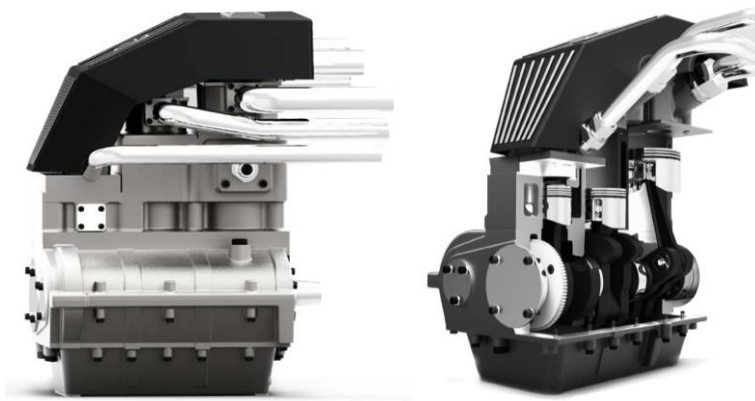


Fig. 34: MDI's engine

Following next the MDI engine and the Di Pietro motor are compared.

5.7.2. Comparison between MDI and Di Pietro engines

Below is presented a comparative table between the MDI engine and the Di Pietro engine.

	MDI engine	Di Pietro engine
Power	72 kW (53,69 HP)	17,15 kW (23 HP)
Torque	230 Nm	115 Nm
Weight	35 kg	9,5 kg
Parts	Over 700 different components	11 main different components
Emissions	Mono-energy mode: Air Dual energy mode: Air, CO ₂ , nitrogen oxides and unburned hydrocarbons	Air

Table 6: Comparison between the MDI engine and the Di Pietro engine.

Although the Di Pietro engine seems to be less powerful than its MDI counterpart, it does not mean it is worst. As seen in this chapter, the Di Pietro engine is capable to fulfill the requirements of the SG9C. And the most important point, which is the environmental impact of the engine, is where the Engineair's motor excels at. To manufacture the engines, the Di Pietro motor requires fewer components and resources than its MDI counterpart. Last but not least, the Mr Di Pietro's engine, unlike the MDI motor, never emits any pollutant gas or particle under any circumstance. It just exhausts air, clean breathable air.

6. The air tanks

In order to run the pneumatic motor, it is compulsory to have a compressed air storage in the vehicle. As petrol cars have the gas tank or electric cars have their batteries, air-powered vehicles have compressed air tanks.

Current air tanks are capable to store air under high pressure, which is desirable in a mobility application like this one. The more pressure there is in a certain closed volume, the more air mass can be stored, and the further distance can travel the vehicle before refilling the bottles with compressed air.

But high pressurized tanks have a counterpart. In case of accident, there could be high risk that the tank explodes depending on the material of which it is made. If the bottles were made of metal, apart from adding a lot of weight to the vehicle, in case of heavy collision and fracture of the tank, it would shatter into lots of small pieces of metal, which would be as shrapnel towards the passengers.

To avoid this catastrophic situation compressed air bottles are made of thermoplastic material wrapped with carbon fibre. This means that in case of rupture, the tank doesn't shatter. It would just crack, remaining as a single piece, and the air would escape through the fissure producing quite loud noise but without any danger for the vehicle occupants. An example of this type of tanks are those regulated by the ISO 11439 normative, which can store compressed air to a pressure up to 300 bar (or even 400 bar in some cases) and between temperatures of -40 °C and +65 °C. The different air tank types and their structures are detailed in its correspondent subsection.

6.1. Previous considerations

The pressure at the output of the tank is considered constant. This means that the losses which would appear as the tank empties and those due to the empty speed of it are neglected.

6.1.1. Thermodynamic air model

In most situations, the conditions of a study allow the researchers to assume that air behaves as a perfect gas. However, at high pressures, such as inside the vessel, this hypothesis is not valid. Thus, a modified version of the equation is used, which is the perfect gas equation corrected with the compressibility factor.

Thus, the formula used is the following one:

$$P \cdot V = \frac{m_{air}}{M} \cdot R \cdot T \cdot Z \quad (\text{Eq. 3})$$

Where P is the pressure of the gas, V is the volume of the gas, m_{air} is the total gas mass, M is the molar mass of the gas, R is the universal gas constant, T is the temperature of the gas and Z is its compressibility factor. If the compressibility factor is isolated, the compressibility factor can be described with the following expression:

$$Z = \frac{P \cdot V \cdot M}{m \cdot R \cdot T} \quad (\text{Eq. 4})$$

The compressibility factor, is the ratio of the ratio of the molar volume of a real gas to the molar volume of the same gas but if considered ideal, at the same pressure and temperature. It is a correction factor which defines the deviation of a real gas from ideal gas behaviour. For this reason, an ideal gas has a compressibility factor of 1, and it increases if the pressure or the temperature increase.

Moreover, air has been considered to be dry. Air could not be supposed to be dry in some applications such as air conditioning, which is not the case, so this assumption does not introduce significant error to this study. See Annex C to consult the compressibility factor tables.

6.2. Air tank types

The air tank used in the vehicle has to fulfill a series of requirements to ensure that it can operate safely, and so the vehicle. But also, the tank has to be as lightweight as possible, so the vehicle does not carry more load than strictly necessary and it does not affect negatively to the autonomy range.

Moreover, it has been thought to use a commercial tank in order to reduce costs, as manufacturing a new one would require a bigger budget for the project.

For these reasons, the air tank type that satisfies all these criteria is the tank that responds to the ISO 11439 normative. This kind of tank is used in the automotive industry for vehicles powered by hydrogen or CNG, which are inflammable substances. Considering that these bottles operate safely with these hazardous fuels, the use of them to store air instead makes the vehicle even safer.

But before selecting a tank, it is necessary to know which types of tanks exist and which characteristics they have. Therefore, following next is presented a brief list of the types of tanks to choose from.

Type I

The Type I tank is made entirely of steel. It is the heaviest tank of the four types and it requires maintenance, as the metal is prone to rust and corrosion. However, due to its simplicity on the materials and the construction, the Type I tank is also the cheapest one.

These characteristics make the Type I tank especially suitable for stationary applications.

Type II

Type II tanks consist in a metallic cylinder wrapped partially with carbon fibre on the side body only. The top and bottom steel ends remain exposed as they are not covered with carbon fibre. The side coating allows the cylinder to have thinner side steel walls, so the Type II tank is lighter than the Type I, but also more expensive.

Type II tanks require maintenance also as the top and bottom exposed steel is susceptible to rust as well.

Type III

This type of tank is, unlike the Type II ones, are fully wrapped with carbon fibre, and the inner metal used is aluminium instead of steel. This feature makes Type III tanks more lightweight (and more expensive as well) than Type II tanks, and obviously than Type I tanks.

Despite this tank type does not have exposed metal, it requires maintenance too, as the inner aluminium is prone to galvanic corrosion.

Type IV

Type IV tanks use the latest technology in the pressure vessel matter. They use a non-metallic polymeric liner fully wrapped with carbon fibre. Thus, this type of tank is the lightest one.

Therefore, this is the most expensive tank type. However, this tank does not need any maintenance, as there is no rust or corrosion because of the non-metallic materials of which the tank is made.

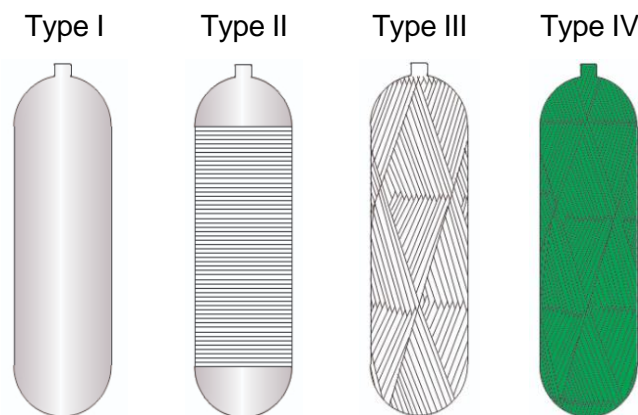


Fig. 35: Type I, II, III and IV tanks internal structure schematic.

Having seen the overall characteristics of each type of tank, it is clear that the selected tank should be the type IV tank. The main reasons to make this decision are two: on one side type IV tanks have the desired properties and performance that fit best for the intended mobility application; and on the other side, type IV tanks do not require maintenance, so it is in fact cheaper than other tank types in the long term.

6.2.1. Characteristics of the selected tank

Once the Type IV tank choice is clear, some further details and features are explained next.

As seen, type IV tanks are lighter than type I, II and III vessels, due to the use of non-metallic polymeric liner fully wrapped with carbon fibre instead of aluminium or steel. This helps to reduce the overall weight of the vehicle and thus, improves its performance.

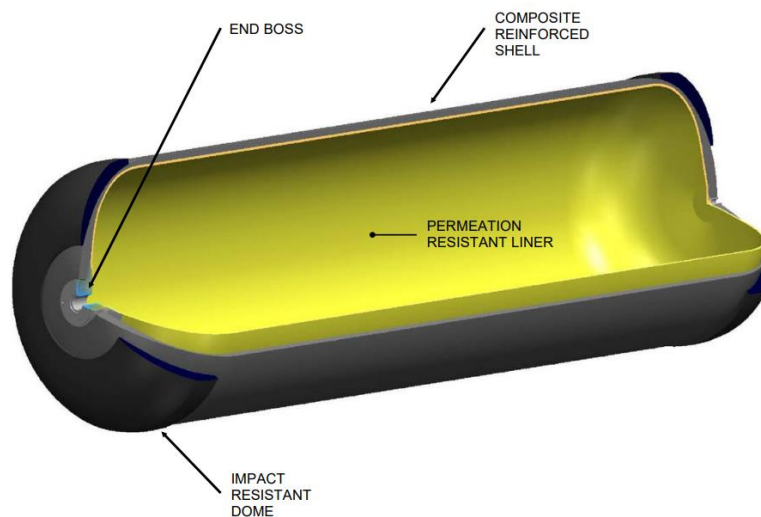


Fig. 36: Internal structure of a type IV tank.

During the manufacturing of this kind of tank, special additives are added to the polymer liner to make it resistant to rust and fatigue. For so, type IV bottles do not rust or suffer any corrosion, which avoids any leakages in the tank.

This last point leads to the fact that type IV cylinders do not require maintenance at all. Moreover, this kind of tanks are expected to have more than 20 years of service life. For these reasons, the use of type IV bottles brings huge savings to its owners.

Obviously, all these commented features are not achieved to expenses of security. Safety is the most important matter. For so, these tanks are designed to be highly safe. These tanks have an outstanding resistance and strength that withstand drops on multiple sides from up to 1,8 m. Moreover, type IV tanks are bullet-proof. The vessels do not shatter when a projectile goes through the pressurized tank. It is

also able to operate safely between the temperature range that comprehends between -40 °C and 65 °C, as commented previously.

Finally, the air properties inside one type IV tank are presented in the table 7.

Pressure	300 bar
Volume	100 L
Temperature	293,15 K (20 °C)
Compressibility factor	1,1036
Air mass	32,3052 kg

Table 7: Air properties inside the one type IV tank.

Knowing these data, to ensure the vehicle has enough energy to have the desired autonomy range, there will be needed 3 air tanks. So, at the end the car will have 300 litres in total of volume to store a total air mass of 96,916 kg.

6.3. Available energy

The available energy inside the tank is a key parameter of the study, as it is directly proportional to the autonomy range of the vehicle. But not all the energy inside the tank is used to make the engine rotate. The useful part of this energy is the exergy.

To visualize better what exergy is, let's imagine a cup of water in equilibrium with the surroundings. This water has an internal energy, but with it is not possible to do any work. However, if the water is very hot or very cold, it has the potential to transform this excess of energy into work.

The formula used to calculate the exergy in the tank is the equation 5.

$$ex = u_1 - u_0 + P_0 \cdot (v_1 - v_0) - T_0 \cdot (s_1 - s_0) \quad (\text{Eq. 5})$$

Where:

- ex is the specific exergy inside the tank expressed in J/kg.
- u is the specific internal energy inside the tank expressed in J/kg.
- u_0 is the specific internal energy at the dead state expressed in J/kg.
- P_0 is the pressure at the dead state expressed in Pa.
- v is the specific volume inside the tank expressed in m³/kg.
- v_0 is the specific volume at the dead state expressed in m³/kg.

- T_0 is the temperature at the dead state expressed in K.
- s is the specific entropy inside the tank expressed in J/kg·K.
- s_0 is the specific entropy at the dead state expressed in J/kg·K.

The dead state is the state of the surrounding environment, which is considered to be the atmospheric pressure $P_0 = 1 \text{ atm} = 101325 \text{ Pa}$ and $T_0 = 20 \text{ }^\circ\text{C} = 293,15 \text{ K}$.

So, considering all these data and the formula just seen above, it can be obtained a specific exergy of $385033,37 \text{ J/kg}$, which is the same as $0,1070 \text{ kWh/kg}$.

This value is the useful energy that will be used to move the motor for each kilogram of air. Thus, the total exergy results of multiplying the specific exergy obtained with the total air mass stored in the tanks. The total exergy of the vehicle is $37,32 \text{ MJ}$, or $10,3655 \text{ kWh}$.

6.4. Tank refilling

The CAV, as electric and petrol vehicles, obviously has no unlimited energy. For this reason, when the air reserves are low, the tank needs to be replenished. But, unlike other propulsion technologies, compressed air tanks can be refilled by two means: from the compressed air equipment at gas stations or at an electric plug.

The scheme of the refilling process is the one following below:

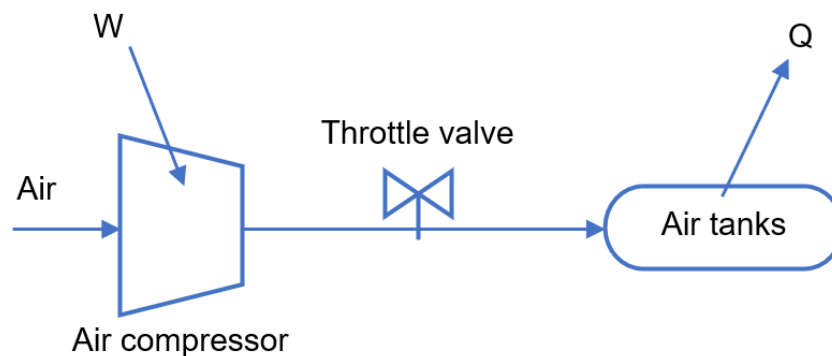


Fig. 37: Tank refilling process.

However, with the current technologies available it is possible to refill the air tanks at the air pump of gas stations in 90 seconds and at a terminal electric terminal or at a home socket in 3,5 hours, according to MDI.

6.4.1. Previous considerations

It has been considered that the air compressor does not have heat loss, but the air tanks do have heat loss. Moreover, when the tanks are empty is considered that in their interior there is air at atmospheric pressure and temperature.

6.4.2. Gas station refilling

The first way to do so is at the gas station. The majority of gas station have air compressors mainly to inflate car's tires. But this infrastructure can be used to refill compressed air vehicles. The procedure is just as if it was fuel instead of air, attaching the compressed air pump to the tank's compressed air inlet. This refilling method does not take more than few minutes.

6.4.3. Plug charging with a provided air compressor

The second manner to refill the air tank is to plug the vehicle to a terminal for electric vehicle charging or to a standard home socket. The electric energy is used by the provided air compressor to fill the tanks. This provided air compressor undoubtedly has less power than an industrial air compressor, so this refilling process takes longer than the previous explained method. This process takes few hours, so it is especially interesting for night charging.

6.4.4. Required work and heat loss

In this subsection are presented the results of the calculations of the required work necessary to refill the tanks completely. As it can be appreciated in the mathematic procedure in the Annex D.3, the heat loss in the air tanks is 2,096 kWh and the required work is 5,791 kWh. This information will be useful for the future work of choosing an air compressor to refill the tanks at home.

6.5. Input Air Temperature effect on autonomy range

In the Engineair's Tech Note sent by its inventor Angelo Di Pietro to the author of this papers it is claimed that heating the air before it enters the engine has huge impact on the autonomy range.

Mr Di Pietro considers that an input temperature of 600 K instead of the almost 300 K proposed can be achieved with a heat source, without any technology change of the device. As an example, the Italian engineer says that considering the standard air consumption of 84 m³/h (101,22 kg/h) with the same pressure but increasing the temperature up to 600 K, the standard air rate consumption will be of just

41,041 m³/h (49,45 kg/h). This statement is demonstrated below in the Annex D.2.

It is been seen that doubling the inlet temperature of the engine reduces by a half the consumption, meaning that the range of autonomy is doubled with the same tank of compressed air.

So, if in a given moment a vehicle with a powertrain like the designed in these papers goes into production, it would be interesting to offer the vehicle with the option of an air heater between the air tank and the Di Pietro motor. Although the vehicle presumably would be a bit more expensive than without the air heater, it would have an extended range of autonomy, specifically the double than the standard vehicle.

7. Autonomy range

In this chapter is intended to do energetic study in order to determine the range of autonomy of the car.

Once the available useful energy to move the engine has been calculated, the next step is to calculate the required energy for the vehicle, so with it can be found the range of autonomy of the SG9C.

7.1. Previous considerations of the autonomy study

To perform an autonomy range study is essential to know the conditions of the study, as the autonomy range highly depends on the driving style. In these papers have been considered two main scenarios: at constant speed and in an urban cycle.

Constant speed driving lacks acceleration and braking. Is an ideal situation where the vehicle is in a permanent kinematic state. This kind of driving barely fits in the environment where a city car moves, but it is a good approximation to interurban road driving. It is also useful to make approximations considering an average speed.

Unlike driving at constant speed, the urban cycle is the most common situation in cities by far. It is characterized by accelerating and braking repeatedly. As the air powered vehicle that pretends to design these papers is a small city car, the urban cycle is especially interesting to study, as it is the closest situation to the reality. For this study it is used the ECE-15 cycle specifically, which is detailed in its subchapter.

Neither cases will contemplate the motorway or highway scenario, as the vehicle is not intended to reach those high speeds.

Moreover, to determine the required energy to move the vehicle, first it is compulsory to know and define the resistant forces and losses that interact with the vehicle, as well as some of its estimated physical and geometrical parameters.

Another consideration to be aware of is that all the elements, except the Di Pietro engine, have been considered ideal. Examples of these elements are the shaft, the air valves, the tank, etc. It has also been considered the transmission relation between the engine and the wheel to be 1:1, so the wheel spins the same as the engine. If not specified, the transmission is 1:1. In case it is not, it will be stated.

7.1.1. Constant speed driving

As commented previously, the constant speed driving is a situation not likely to occur in city environments. However, this kind of study is useful when the speed is in fact an average speed. Depending on the circumstances of the driver and the traffic, the average speed of a vehicle during a certain period of time can vary in a huge range of different speeds.

7.1.2. Urban cycle

The urban cycle of this study is the ECE-15, a standardized European urban cycle. This cycle simulates a city focused style of driving in stop-start traffic. The profile of this cycle is appreciated in the figure 38. It is divided in three main sections, each one described below:

- Section A:
 - 1. From 0 to 15 km/h in 5 seconds.
 - 2. Maintain speed at 15 km/h for 10 seconds.
 - 3. From 15 to 0 km/h in 5 seconds.

- Section B:
 - 1. From 0 to 30 km/h in 10 seconds.
 - 2. Maintain speed at 30 km/h for 30 seconds.
 - 3. From 30 to 0 km/h in 10 seconds.

- Section C:
 - 1. From 0 to 50 km/h in 25 seconds.
 - 2. Maintain speed at 50 km/h for 10 seconds.
 - 3. From 50 to 35 km/h in 5 seconds.
 - 4. Maintain speed at 35 km/h for 10 seconds
 - 5. From 35 to 0 km/h in 10 seconds.

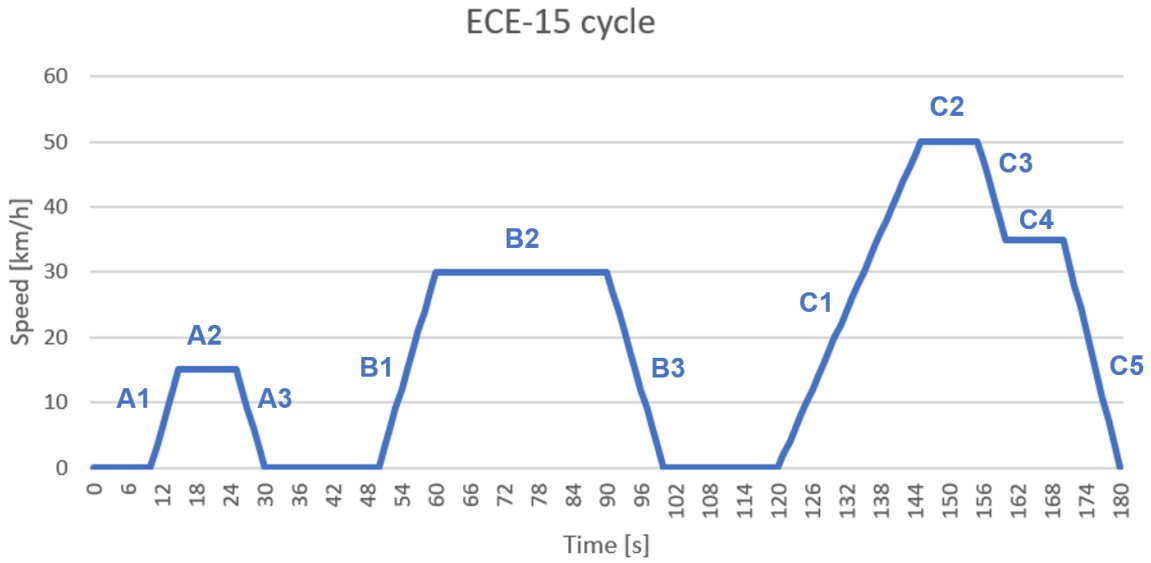


Fig. 38: ECE-15 urban cycle.

Although this is a variable speed situation, in order to simplify the calculus process without introducing significant error, it can be mathematically considered as constant speed. From the cycle can be obtained the average speed, so the procedures used in the constant speed sections can be used here as well.

7.1.3. Passive resistances

The forces in the vehicle are related by Newton's Second Law:

$$\Sigma F = m_{total} \cdot a \quad (\text{Eq. 6})$$

If the different forces are disaggregated the expression is as follows:

$$F_t - (F_w + F_r + F_g) = m_{total} \cdot a \quad (\text{Eq. 7})$$

Where F_t is the tractive force, F_w is the aerodynamic friction losses, F_r is the rolling friction losses, F_g is the hill climbing force, m is the vehicle mass and a is the acceleration.

The total mass of the vehicle considered in the study is formed by the mass of the vehicle (without passengers or cargo), the mass of the passengers and the mass of the cargo. Moreover, the mass of the "empty" vehicle is composed by the mass of the vehicle with air tanks empty and the onboard compressed air mass. Below there is the mathematic expression that represents this.

$$m_{total} = m_{veh} + m_{passengers} + m_{cargo} \quad (\text{Eq. 8})$$

$$m_{veh} = m_{unladen} + m_{air} \quad (\text{Eq. 9})$$

In the table 8 are listed all the concerned masses.

m_{unladen} [kg]	m_{air} [kg]	$m_{\text{passengers}}$ [kg]	m_{cargo} [kg]	m_{total} [kg]
340	97	149	14	600

Table 8: Mass distribution of the vehicle.

The unladen mass of the vehicle (m_{unladen}) has been fixed at 340 kg arbitrarily, which is less than the maximum unladen mass for a L7e vehicle intended for passenger transportation. The air mass stored in the tanks is the one obtained in the chapter 6.2. As the vehicle is a two-seater, the mass of the passengers has been considered the sum of the Spanish female average weight (66,6 kg) and the male average weight (82,4 kg), which equals to 149 kg. Finally, the cargo mass has been fixed at 14 kg, which would be a good amount of cargo considering that the vehicle is a city car and it is intended for passenger transportation, not the carrying of goods. As seen, all these masses are the ones of a worst-case scenario, so most of the time the real car would weigh less than 600 kg and the results obtained would be better than the ones presented in these papers.

Returning to the forces matter, the total force the vehicle has to overcome is shown in the equation 10, and it is the sum of the aerodynamic friction losses (F_w), the rolling friction losses (F_r) and the hill climbing force (F_g).

$$F_{\text{losses}} = F_w + F_r + F_g \quad (\text{Eq. 10})$$

Each one of the forces in the formula represent a different type of loss, which will be briefly detailed in the following subsections.

7.1.3.1. Aerodynamic friction losses

These forces are caused basically by two phenomenona: the viscous friction of surrounding air and the pressure difference in front and rear.

$$F_w = \frac{1}{2} \rho A_f c_d (v_{\text{veh}} - v_w)^2 \quad (\text{Eq. 11})$$

Where ρ is the air density, A_f is the frontal area, c_d is the aerodynamic drag coefficient, v_{veh} is the vehicle speed and v_w is the component of wind speed on the vehicle moving direction.

Note that the v_w term has a positive sign when this component is in the same direction of the vehicle speed and a negative sign when it is opposite to it. However, in the whole study are considered situations with no wind, so $v_w = 0$ m/s.

As the equation shows, the design parameters that can be controlled in the design of the car are the frontal area (A_f) and the aerodynamic drag coefficient (c_d). According to the 3D model made of the hypothetical chassis of the vehicle (see chapter 8.3), the frontal area is $A_f = 1,98 \text{ m}^2$.

The drag coefficient cannot be measured as it would be needed the physical prototype built. However, there it has been seen that the Citroën Ami has a drag coefficient equal to 0,4, so the drag coefficient should be this one at least.

Nevertheless, to compensate other possible losses and assumptions made along these papers, the frontal area will be considered equal to 2 m^2 and the drag coefficient equal to 0,5.

7.1.3.2. Rolling friction

The rolling friction depends on the surface conditions, as well as the tyre pressure and vehicle speed.

$$F_r = f_r m_{total} g \cos(\alpha) \quad (\text{Eq. 12})$$

Where f_r is the rolling friction coefficient, m is the vehicle mass, g is the gravity constant ($9,81 \text{ m/s}^2$) and α is the road slope. If it is not said the contrary, the road slope will be considered 0, which is flat surface.

Rolling Resistance Coefficients	
Conditions	Rolling Resistance Coefficient
Car tires on a concrete or asphalt road	0,013
Car tires on a rolled gravel road	0,02
Tar macadam road	0,025
Unpaved road	0,05
Field	0,1 – 0,35
Truck tire on a concrete or asphalt road	0,006 – 0,01
Wheel on iron rail	0,001 - 0,002

Table 9: Rolling resistance coefficients depending of the surface.

The constant values given in the table 9 do not take into account their variations with speed. However, there are empirical formulas based on experimental results to calculate the rolling resistance on a hard surface.

The rolling resistance coefficient can be considered as a linear function of speed. The equation 13 is suitable for a passenger car driving on a concrete road and predicts with acceptable accuracy the rolling

resistance coefficient (f_r) for speeds under 128 km/h, which is the case.

$$f_r = 0,01 \left(1 + \frac{v_{veh}}{160} \right) \quad (\text{Eq. 13})$$

For the reasons explained earlier the rolling resistance coefficient will be considered variable according to the equation 13. As it can be appreciated in the graphic below, for a speed ramp input from 0 to 50 km/h it can be represented all the rolling resistance coefficient values. The $f_r = 0,013$ estimation is not bad, but seeing that it is in fact only true when the speed is 48 km/h, it is more accurate to utilise the mentioned formula.

In the image below it can be appreciated the value of the rolling resistance coefficient for every different speed between 0 and 50 km/h.

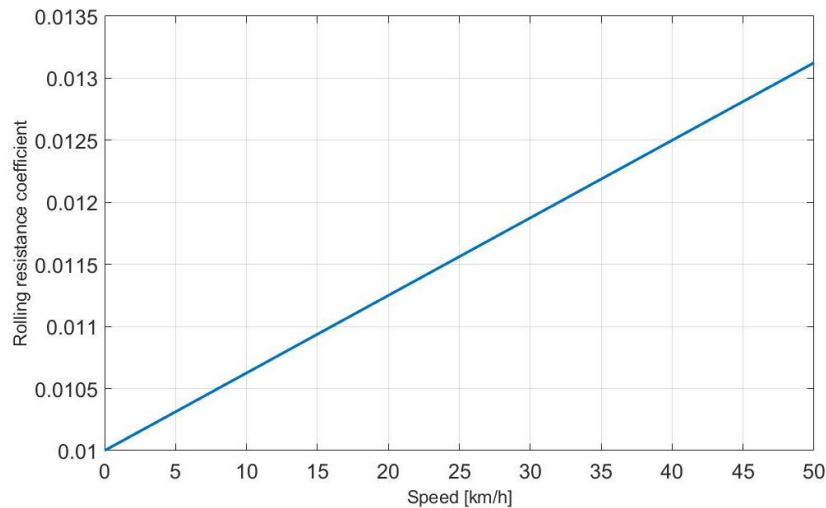


Fig. 39: Rolling resistance coefficient as a function of speed.

7.1.3.3. Hill climbing force

This is the force due to the weight of the vehicle when it is a surface with a certain slope.

$$F_g = m_{total} g \sin(\alpha) \quad (\text{Eq. 14})$$

Where as well as before m is vehicle mass, g is the gravity constant and α is the road slope.

7.2. Autonomy range without considering the engine

In this section is intended to define the energy that the vehicle requires without taking into account the air consumption of the engine.

The required energy will be given by the driving style and the environment conditions, such as the grade of the road or the road's surface. To determine it, a MATLAB and Simulink program has been developed to make the calculus process more agile, which can be found in the electronically submitted files.

Once the tractive required energy (E_t) is calculated, the next step is to quantify the energetic consumption (C) of the vehicle given a known distance (X), by the means of the equation 15.

$$C = \frac{E_t}{X} \quad (\text{Eq. 15})$$

At this point is it possible to determine the theoretical autonomy range of the vehicle with the formula 16, known the energy stored in the tank (which is the exergy seen previously) and the air consumption.

$$AR_{theoretical}^* = \frac{Ex}{C} \quad (\text{Eq. 16})$$

Finally, the real autonomy range will take into account the efficiency of the motor, as shows the equation 17.

$$AR_{real}^* = A_{theoretical}^* \cdot \eta \quad (\text{Eq. 17})$$

7.2.1. At constant speed

Applying the procedure seen above, it can be obtained the autonomy range for different speeds. The duration of the simulation has been fixed as 180 seconds arbitrarily, the engine has 94,5% efficiency and just as a reminder, the available useful energy to power the vehicle is 10,37 kWh.

Thus, the following table has been obtained for different speeds within the range of this quadricycle.

v	E_t	C	$AR_{theoretical}^*$	AR_{real}^*
[km/h]	[kWh]	[kWh/km]	[km]	[km]
10	0,00934	0,0187	554,78	524,27
20	0,02365	0,0237	438,29	414,18
30	0,04685	0,0312	331,87	313,62
40	0,08289	0,0414	250,10	236,35
50	0,13570	0,0543	190,96	180,46

Table 10: Autonomy range for different constant speeds without considering the air consumption of the engine.

However, is it clear that not considering the air consumption of the engine introduces very significant error to the study.

7.2.2. ECE-15 cycle

In the figure 40 it is shown a graphic of the required energy with and without regenerative braking in the ECE-15 cycle. Although the regenerative braking is not considered in this study, it is displayed, so it can be compared the effect of it.

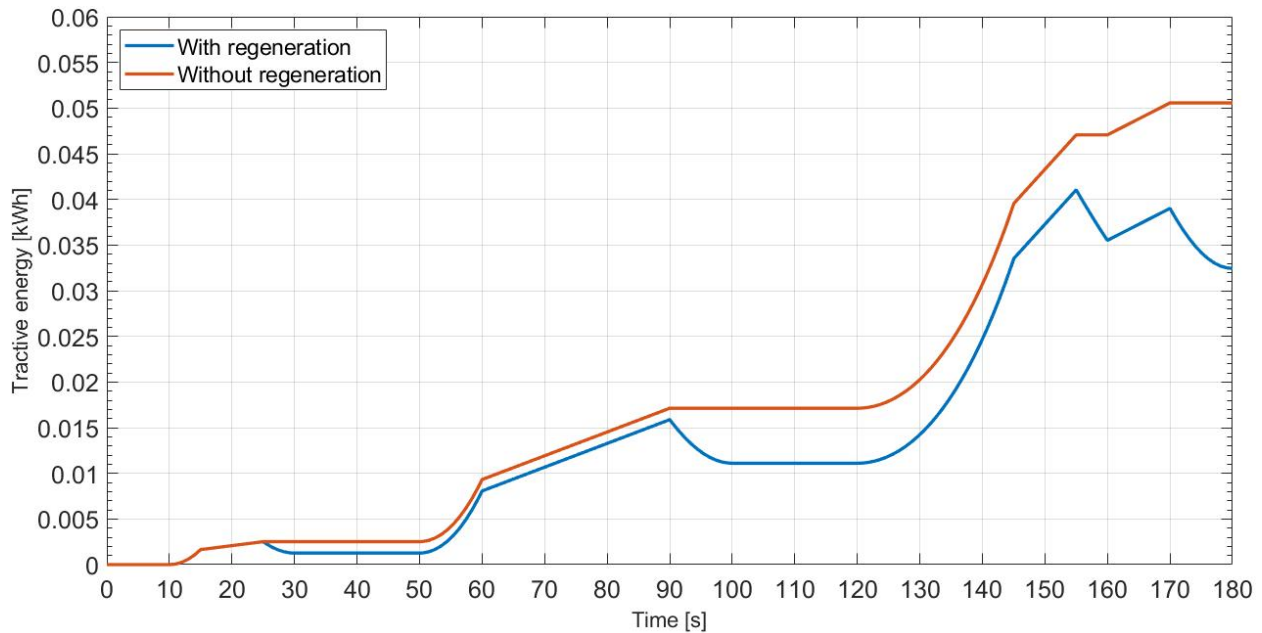


Fig. 40: Required energy with and without regenerative braking in the ECE-15 cycle.

As it can be sensed in the previous graphic, the required tractive energy for an entire ECE-15 cycle is 0,05056 kWh, which is 182,016 kJ, while in the case of regenerative braking the required energy is 0,03244 kWh, which is 116,784 kJ. From the graphic is obtained the table 11.

v	E_t	C	$AR_{\text{theoretical}}^*$	AR_{real}^*
[km/h]	[kWh]	[kWh/km]	[km]	[km]
ECE-15 with regenerative braking	0,03244	0,0355	291,79	275,75
ECE-15 without regenerative braking	0,05056	0,0554	187,22	176,92

Table 11: Autonomy range for the ECE-15 cycle without considering the air consumption of the engine.

However, as commented previously, this calculated real autonomy is not the actual range of autonomy of the car. If the vehicle was electric, the value just obtained would be valid, but in the case of the compressed air vehicle, the autonomy range is subjected to the energy stored in the air tank and the air consumption of the pneumatic engine. For this reason, in the next section is determined the actual autonomy range, which depends on the engine air consumption.

7.3. Autonomy range considering the engine air consumption

According to the extrapolated air consumption graphic viewed in the chapter 5 (see figure 32), assuming the validity of the air consumption hypothesis previously made, it can be calculated the range of autonomy of the vehicle.

In the supposed case that the engine and the wheels of the vehicle rotate at the same speed (1:1 ratio), if a 5 bar (500 kPa) pressure is applied at the inlet of the engine and it rotates at 500 rpm (52,36 rad/s), the air consumption would be of 758 standard litres per minute (STL/min).

Standard litres are, as its name indicates, the volume in litres occupied by a gas at standard conditions, which are a pressure of 1 bar and a temperature of 273,15 K (0 °C). The density of air at those conditions is 1,27537 kg/m³, which means that the air consumption of 758 STL/min is 966,73 g/min.

Considering that the tyre has a diameter of 0,5 m, if it has an angular speed of 500 rpm the speed of the car would be 47,12 km/h.

7.3.1. At constant speed

To obtain the autonomy at constant speed the calculus process starts with the engine's air consumption equation, which is the following:

$$AC = 0,0208947 \cdot P_{in} \cdot \omega \quad (\text{Eq. 18})$$

Where AC is the engine air consumption expressed in STL/min, P_{in} is the engine inlet air pressure expressed in psi and ω is the engine angular speed expressed in rpm.

From this point, following the procedure detailed in the Annex E.2, it is obtained the autonomy formula seen in the equation 19.

$$AR = 5,18324735271 \cdot 10^{-3} \cdot \frac{V_{STL}}{P_{in}} \quad (\text{Eq. 19})$$

With this formula is possible to plot the autonomy range curves for constant speed driving, which can be appreciated in the following two graphics.

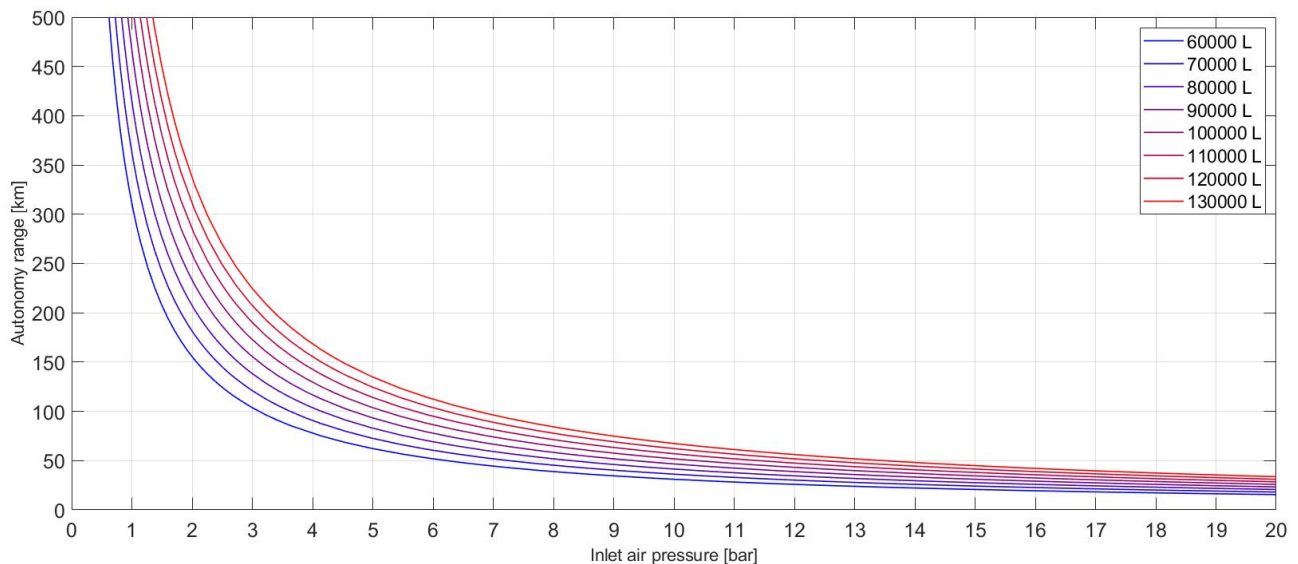


Fig. 41: Theoretical autonomy range as a function of inlet air pressure considering the air consumption of the engine for different tank volumes expressed in STL.

To understand this graphic is necessary to remind that the inlet pressure of the engine is directly proportional to the speed that rotates the engine (assuming the air flow constant), and hence the speed of the vehicle. For this reason, if the inlet air pressure is constant, so does the vehicle's speed.

Each curve represents the range of autonomy of the vehicle if the vehicle drives at the constant speed specified by the constant inlet air pressure. There is a different curve for each different amount of air stored in the tanks, which instead of being expressed in mass units it is expressed in standard litres. Just as a reminder, a standard litre is the volume that occupies a certain mass of gas in normal conditions, which are a pressure of 1 bar (100 kPa) and a temperature of 0°C.

As the graphics show, the more air is stored in the tanks, the more autonomy range has the vehicle. Moreover, the less the inlet pressure is, the more the range of autonomy is, as less inlet air pressure means less air consumption.

Having seen that the mass of air stored in the air tanks is 96,916 kg, this mass in normal conditions occupies a volume (expressed in standard litres) of 75987,49 STL. The autonomy range graphic of the vehicle with these conditions considered is the following one.

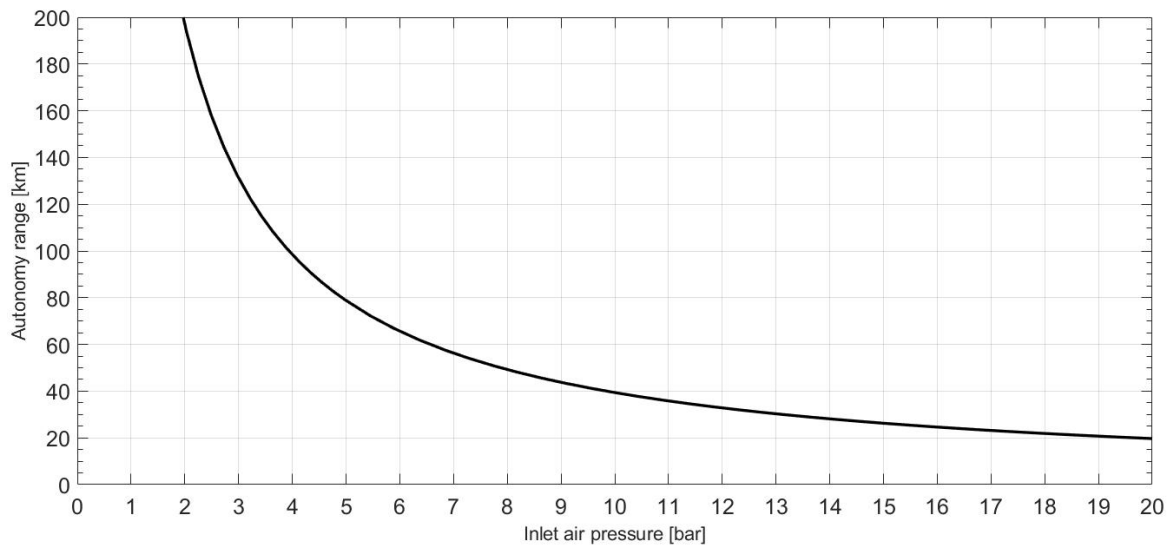


Fig. 42: Autonomy range as a function of inlet air pressure.

It is seen that the results obtained, although they are based in the assumptions commented throughout these papers, have a high validity, as they are very similar to the range of autonomy of the concept vehicles and built prototypes equipped with the Di Pietro engine for a certain interval of inlet air pressures.

7.3.1.1. Effect of different transmission relations

If it is considered a different transmission relation, this causes the wheel to spin faster or slower than the engine. Considering the first case, in which the wheels of the vehicle rotate faster than the engine, bigger autonomy ranges can be achieved.

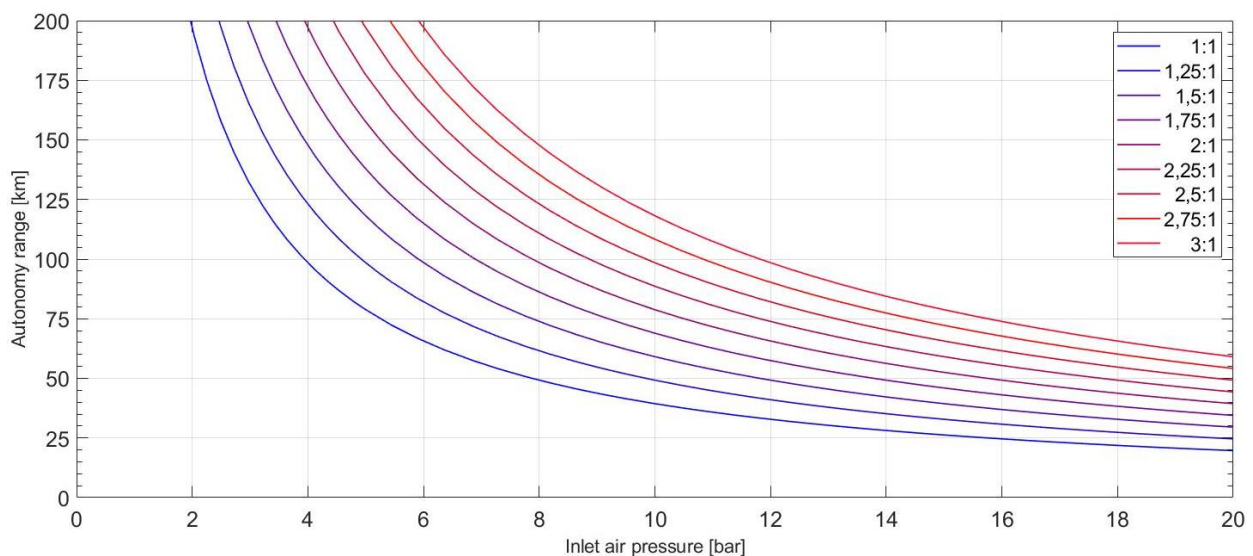


Fig. 43: Autonomy range curves for different transmission relations.

As seen in the figure above, the autonomy range increases as the relation of transmission increases. This happens because with the same number of revolutions of the Di Pietro engine, the wheel covers

more distance. However, this is not an infinite growth, as physical restrictions and impediments will occur more toughly the more the transmission relation increases. This serves to see that a minimum range of autonomy of 50 km is possible, as it would be the range for the maximum inlet pressure applied of 20 bar (2 MPa).

7.3.2. ECE-15 cycle

In this subsection, the autonomy range would have been evaluated with the ECE-15 urban cycle. However, due to its calculus complexity, the results of this part of the study have been obtained in a different way. This case has been considered as a constant speed scenario with the average speed of the ECE-15 cycle. With this methodology, the results are valid as well without the necessity to develop unnecessarily complex mathematical procedures.

For so, the results obtained in this case are the same ones of the section 7.3.1. because the average speed of this urban cycle is 18,35 km/h, which is between the range considered in the study.

8. The SG9C

In this section it is described briefly how the urban vehicle powered with the powertrain designed should be in order to be the one of the most useful tools in the automotive industry to fight climate change.

8.1. Powertrain scheme

The final scheme of the powertrain is the following presented in the figure 44. The dashed rectangle symbolizes the vehicle. For so, all the elements of the powertrain are inside the dashed rectangle, except the air compressor, which would be outside the vehicle.

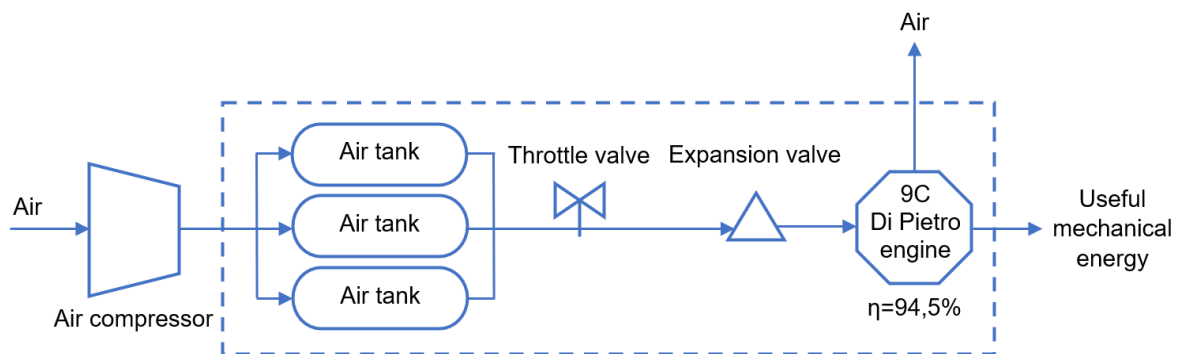


Fig. 44: SG9C's powertrain scheme.

As the scheme shows, the main components are:

- The Di Pietro engine, which has been deeply analysed previously and it is the element that powers the vehicle.
- The air tanks, which have also been studied in these papers and they have been decided to carry nearly 97 kg of compressed air.
- The throttle valve, which is would be used to control the mass flow of air, and thus, the speed of the Di Pietro engine.
- The expansion valve, which controls the inlet air pressure without varying the air mass flow.
- The air compressor, which would be used to refill the air tanks at the owner's homes.

8.2. Chassis and body

The figure 45 is the internal tubular structure of the Green'air, the golf cart prototypes designed for MDI. The SG9C should have a chassis with similar tubular frame, but logically adapted to its different shape. To reduce weight the tubular frame is thought to be made of aluminium, although this analysis is intended for future work.



Fig. 45: Internal structure of MDI's prototype Green'air.

There is thought of two different bodies that would surround the tubular frame. On the one hand there is the body made of composites, as these materials have a very high resistance to weight ratio. Examples of composites are polyurethane foam or fibreglass, which combined give as a result an even better chassis than with these materials by separate. This option is the one that offers a better performance, but it also is more expensive than the other option that is presented next.

On the other hand, there is the body made of polycarbonate, a polymeric material. The main advantage of this kind of materials is their low costs and the easiness to mould the material in the desired shape. This kind of polymer is also recyclable, although the process to do it costs more than with thermoplastics. However, nowadays more companies are increasing their effort to improve the recycling process of polycarbonates, so it is expected to become easier through the years.

8.3. 3D model

As commented in the market research chapter where the Citroën Ami is explained, an efficient way to reduce costs is to make the vehicle double symmetrical. This means that the vehicle has two perpendicular planes intersection of which is just a vertical line located in the middle of the vehicle. In other words, from the exterior the front and back chassis panels are the same, and the right and left door are the same. This last condition imposes that one door opens forward and the other backwards.

In the following image is showed the 3D model of the SG9C created with the SolidWorks CAD software by Dassault Systèmes.

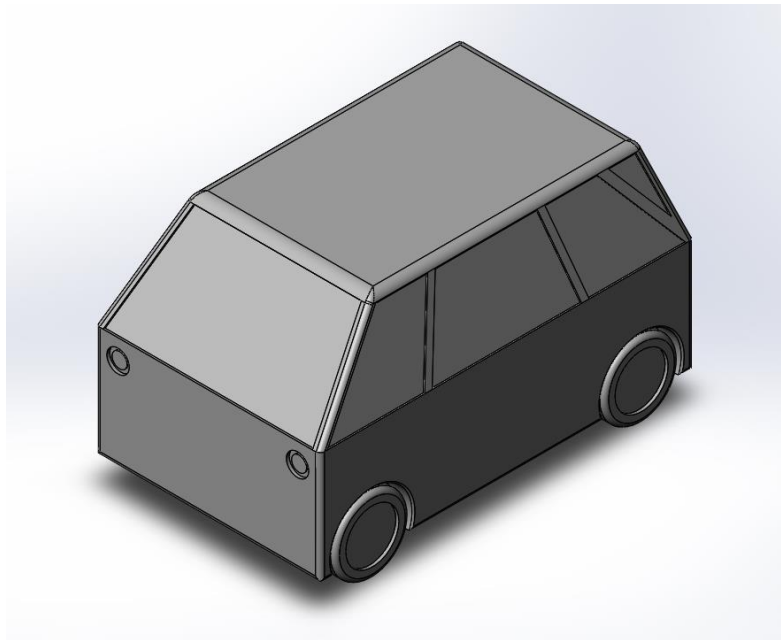


Fig. 46: SG9C 3D model.

As it can be noticed in the figure 46, the SG9C does not seem to fulfill these symmetry conditions. This is because the symmetrical part is the whole vehicle except the triangular prism shaped part of the back. This feature adds practicality to the vehicle, as it has a little more interior space, and it gives also an aesthetic enhancement, as it is clear which part of the vehicle is the front and which one is the back. These has been planned this way as one of the main criticisms to the Citroën Ami is its confusing aspect.

8.4. Refilling process

As commented in previous sections there are two different ways to refill the air tanks. The first one consists in directly refilling the tanks directly from the air pump that most gas stations have.

In order to make even easier the refilling process for the SG9C's users, it has been thought an innovative way to refill the tanks. It basically consists in replaceable tanks. The chassis panels should have a design which allow to disconnect and remove the empty tanks from the vehicle, so then they could be replaced instantly by fully filled ones. This application would be interesting in both applications, either at home refilling or at gas stations.

The possibility of having this feature in the vehicle would carry some advantages and disadvantages. In one hand, the main advantage of the vehicle is that the SG9C could be refilled immediately. There would be no need to wait for the tank to be full again, as the empty ones are just swapped for already full vessels.

On the other hand, this feature would increase the overall cost of the vehicle because not only the on-

board tanks are supplied to the customers, but also extra ones to make the tank swap possible. Moreover, some sort of device would have to be supplied as well to help owners to carry and replace the heavy vessels.

It has to be noticed that this application is a possible way intended to avoid the long charging times of at home tank refilling. The tank replacing would also be possible at the gas station, but less interesting as the refilling time is already remarkably short.

If this system was feasible, the refilling experience for the users of the quadricycle would be easier, more practical and more flexible.

8.5. SG9C technical specifications

8.5.1. Vehicle theoretical maximum speed

As it has been seen in previous chapters, the Di Pietro motor is a scalable engine, which means that the engine can offer more or less power regulating the air pressure input with a valve.

To determine the theoretical maximum speed of the vehicle the calculations have as a starting point Newton's Second Law, from which the tractive force has been isolated. Knowing that the engine power is the tractive force times vehicle speed, an expression of the power of the engine depending on the velocity of the vehicle can be obtained. To consult the calculus procedure, see Annex F.3, which gives as a result the equation 20.

$$P_t = F_t \cdot v_{veh} = \frac{1}{2} \rho A_f c_d (v_{veh} - v_w)^3 + f_r m_{total} g \cos(\alpha) v_{veh} + m_{total} g \sin(\alpha) v_{veh} \quad (\text{Eq. 20})$$

As it can be appreciated in this formula, the air consumption of the engine is not considered here, which is why the achievable maximum speeds are actually lower than the ones showed in the graphics coming up next.

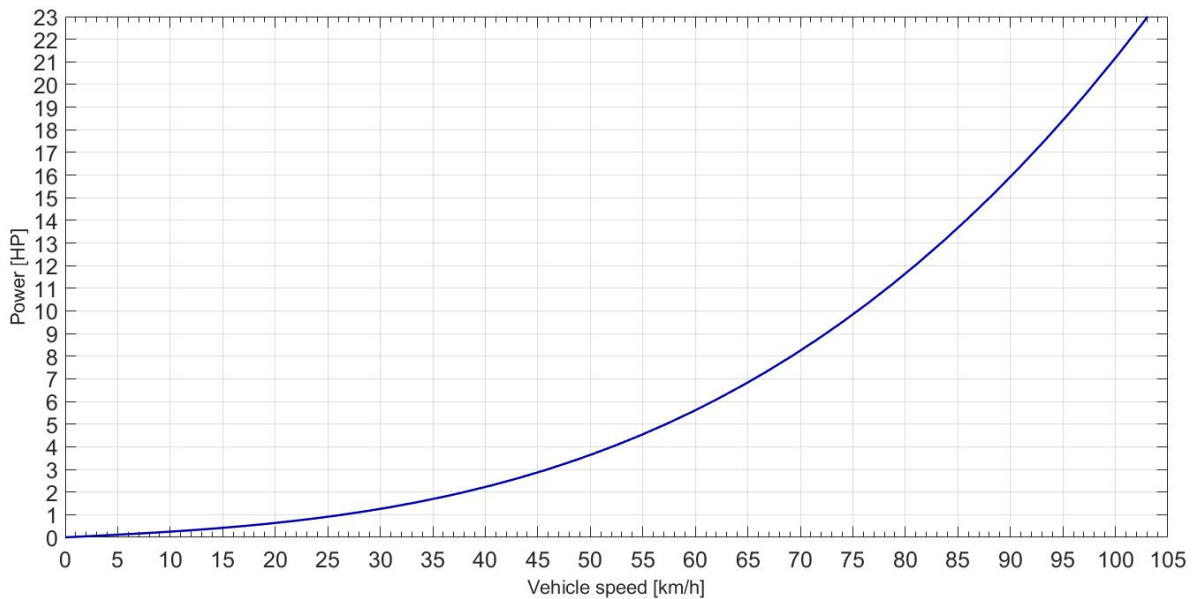


Fig. 47: Theoretical maximum vehicle speed on flat surface.

This graphic is read as for each power of the engine a theoretical maximum speed of the vehicle is obtained. Just as a reminder, the power of the engine is given by the inlet air pressure, as seen in previous chapters.

The values seen in the figure 47 are obtained only considering the aerodynamic friction losses and the rolling resistance losses. Other factors like the engine's efficiency, the power loss due to the differential transmission or some other miscellaneous losses have not been contemplated here. Moreover, these numbers have been calculated under the assumptions of flat surface (no grade, $\alpha=0$) and no wind ($v_w=0$). For all these reasons, these values are not achievable. Obviously, as commented previously, the acceleration is equal to zero ($a=0$).

Furthermore, the top speeds of some of the prototypes seen previously just reflect that the vehicle that is being designed in these papers cannot reach numbers like those. However, let's not forget that lower speeds are more than enough for the urban vehicle, which will drive mainly for city or town roads where have speed limits of 30, 20 or even 10 km/h. Just remember that the Citroën Ami has a top speed of 45 km/h, which the SG9C is able to exceed.

However, if the road grade is considered (uphill slope), the maximum speed is logically decreased. As it can be appreciated in the figure 48, as the road slope increases, the maximum speed decreases dramatically. Here the grade of the road has been considered between 0% (flat surface) and 20%, which the equivalent angles expressed in degrees are 0° and $11,31^\circ$ respectively. As before, in real life these velocities would be lower than the ones represented on the graphic.

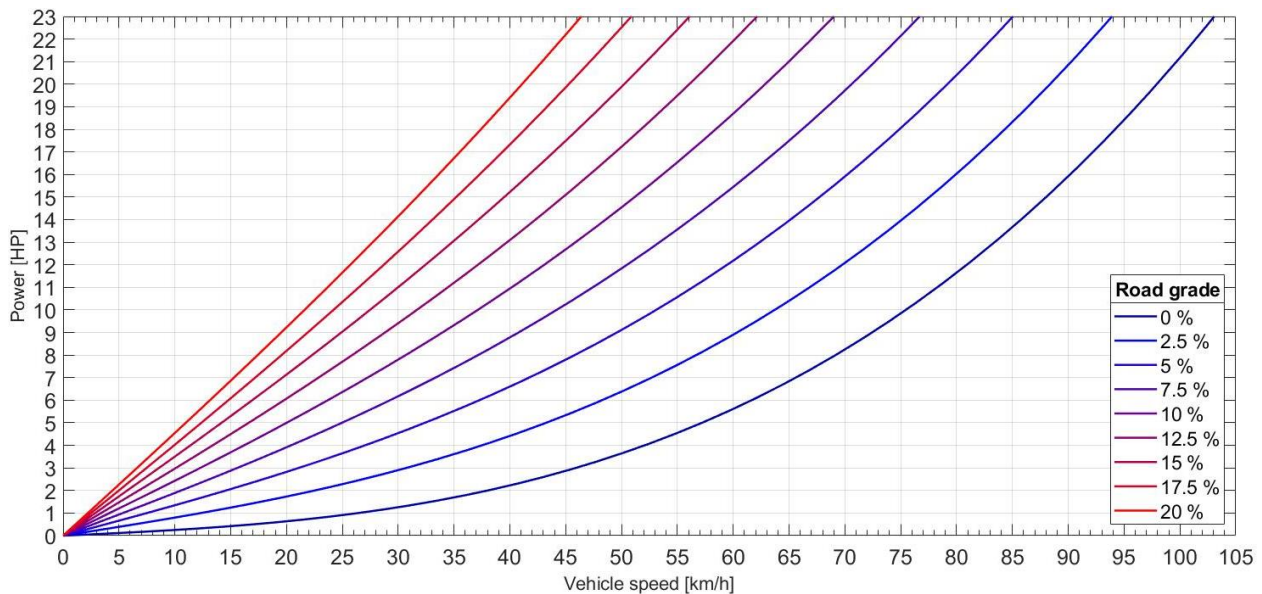


Fig. 48: Maximum theoretical vehicle speed in function of the engine's power.

The utility of this graphic is to show the reduction of the maximum speed due to the slope of the road. For instance, if the graphic says that in a flat surface the vehicle could reach 103 km/h and with a 15% slope the vehicle could reach 56 km/h, the top speed has reduced a 54%. This means that although these speeds are higher than the real ones, the speed reduction would be 54% as well with the real speeds.

For so, as the real maximum speed of the vehicle would be 50 km/h, as seen in previous chapters, the maximum speed with a 15% grade should be expected to be around 25 km/h.

The road grade has been chosen as so because 20% road slope is the maximum grade of a ramp that can be found in a city. With this range of grades, it can be evaluated some common situation in daily city driving, although it is rarer to find grades between 10% to 20%. For instance, parking ramp slopes are preferred to have a 5% grade or less, even though slopes up to 7% are tolerated in urban areas with high density. Non-parking ramps are recommended to have a maximum slope between 12% and 14%, but in some cases slopes up to 20% are considered. For this reason, the maximum grade studied has been 20%.

8.5.2. Pressure loss in the pneumatic tubes

Jaroslaw Zwierzchowski made an estimation of the supply parameters of a working chamber with some flow simulations. If these simulations are valid and based on true premises and assumptions, the working chamber supply parameters are the following indicated on table 12.

Parameter	Value
Pressure [bar]	3
Air speed [m/s]	13,5
Mass flow [kg/s]	0,018
Volumetric flow rate [L/s]	4,97

Table 12: Working chamber simulated supply parameters.

If this situation is considered to be happening in the pneumatic tubes as well, the pressure losses can be estimated. It must be clear that this simulation represents just one situation above all the possible situations while driving a vehicle powered by Engineair's motor.

Firstly, assuming the hypothesis that air can be considered as incompressible, it can be used the flow formula (equation 21) to determine the diameter of the tube considered in the simulation.

$$Q = A_{pipe} \cdot v_{air} = \pi \cdot \frac{D^2}{4} \cdot v_{air} \quad (\text{Eq. 21})$$

This hypothesis will be confirmed or denied following next. As a result, the diameter of the pipe obtained is $D=0,02165 \text{ m} = 21,65 \text{ mm}$.

Assuming the validity of the numbers in the chart above, it can be determined the air behaviour by the means of the Reynolds and Mach dimensionless numbers. If $Re < 2300$, air behaves as a laminar fluid; if $2300 < Re < 4000$, air the air is in transition state, and if $Re > 4000$ air behaves as a turbulent fluid. With the equation 22 the Reynolds number is obtained.

$$Re = \frac{v_{air} \cdot D}{\nu} \quad (\text{Eq. 22})$$

Considering that the kinematic viscosity is $\nu = 5,1029 \cdot 10^{-6} \text{ m}^2/\text{s}$, the resultant Reynolds number is $Re = 57277,60$, which clearly means that air has a turbulent behaviour.

Moreover, with the Mach number it can be determined if air can be considered incompressible or compressible. If $Ma < 0,3$, the fluid is incompressible, whereas $Ma > 0,3$ means that the fluid is compressible. Moreover, if $Ma < 1$, the fluid is considered subsonic, whereas $Ma > 0,3$ means that it is supersonic. The Mach number is calculated with the following formula (equation 23).

$$Ma = \frac{v}{v_{sound}} \quad (\text{Eq. 23})$$

Thus, knowing that speed of sound is approximately 343 m/s, it is obtained a Mach number of

$Ma=0,0394$. This means that the air that circulates through the pipes has to be considered as incompressible and subsonic, as the Mach number obtained is lower than 0,3 and logically lower than 1. The hypothesis of considering air incompressible inside the pneumatic pipes has been confirmed.

To determine the pressure drop, is it compulsory before to calculate the friction factor of the pipe. To do so, the relative pipe roughness and Reynolds number are needed. The diameter of the pipe has been found to be 21,65 mm, and the absolute pipe roughness (ϵ) is 0,0015 mm, the one of a plastic pipe.

$$\text{Relative pipe roughness} = \frac{\epsilon}{D} \quad (\text{Eq. 24})$$

Using the equation 24 the relative pipe roughness is $6,9284 \cdot 10^{-5}$. Using the Moody Diagram (see Annex F.2) can be obtained the friction factor, which result to be $\lambda=0,02054$.

In these calculations are only considered the pressure drop due to linear tubes because the internal pneumatic circuitry of the vehicle is not determined. The pressure drop due to the friction between the pipe and the air through 1 m of linear pipe section is the following.

$$\Delta h_{linear} = \lambda \cdot \frac{L}{D} \cdot \frac{c^2}{2g} \quad (\text{Eq. 25})$$

The linear pressure drop is $\Delta h_{linear}=8,8124$ meters of air column, which expressed in SI units this pressure drop is $\Delta h_{linear}=313,0957$ Pa, which equals to 0,00313 bar. So, is it fair to say that pressure losses inside the pneumatic pipes are negligible and have no significant effect on vehicle's performance.

However, it remains as future work to design the internal cabling of the vehicle and analyse the pressure drop inside the pipes with their final geometry.

9. Environmental study

9.1. Current situation

9.1.1. Existing alternative solutions

Electric vehicle (EV)

It is the most known alternative to petrol cars. Almost all car manufacturers are betting in some way their future to the electric car.

EVs are thought to be the best solution to climate change, but are in fact more of an intermediate step to a fully carbon neutral mobility scenario. Because if an EV is recharged with electricity generated by coal burning, this is a not very sustainable situation.

Some studies have pointed that the manufacture of an EV can produce more GHG emissions than the manufacture of a petrol-powered car. This is due to the battery of the EV, which needs extra energy compared to the petrol vehicle.

However, the balance tips in favour of the EV if the whole lifetime of the vehicle is taken into account, as the total GHG emissions associated to EVs on average are lower than those related to petrol cars because EVs don't have tailpipe carbon emissions. These emissions are from the manufacturing, charging or refuelling and driving (operation).

So, although EVs are cleaner than petrol cars, it has been shown that they are not clean by far. It has been pointed out the extra energy used to manufacture the batteries of EVs, but not the raw materials used in them, which is also an issue. The batteries of electric cars are made of rare metals, like lithium and cobalt. Cobalt, for instance, is used to give stability to the batteries, so they can operate safely. 56% of the cobalt produced worldwide is used for electric car batteries. Each battery has between 4 and 30 kg of cobalt. This rare metal can be found in many countries around the world, but 70% of it comes from just one country: the Democratic Republic of Congo.

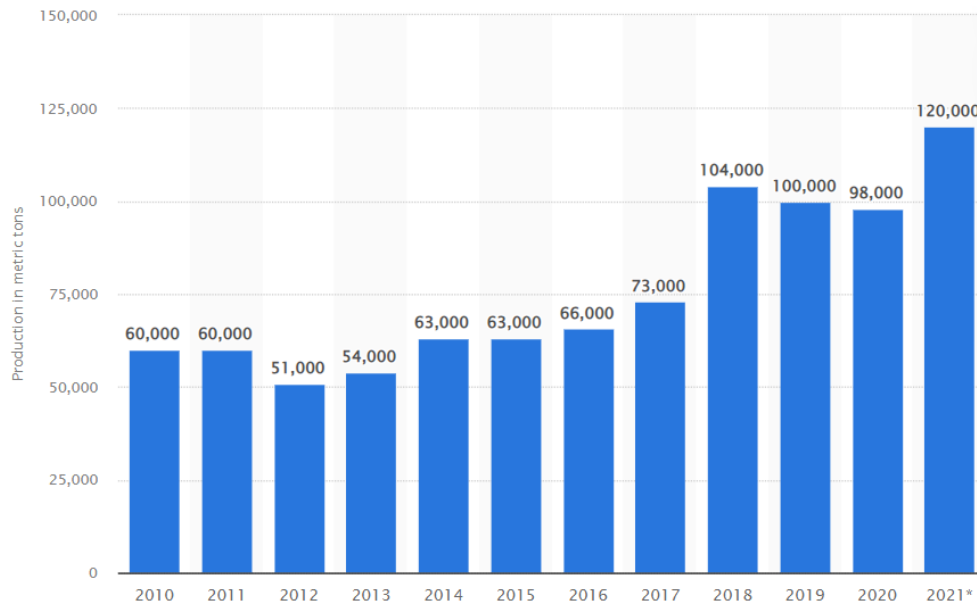


Fig. 49: Annual cobalt production of the Democratic Republic of Congo.

In DRC between 20% and 30% of cobalt production is produced in artisanal mines, in which there are no labour laws, no safety protocols. In these mines work 200000 people. 40000 of them are children, some as young as 6 years old. It is estimated that 2000 illegal miners die every year in Congo, or what is the same, there are 5,48 deaths per day.

China owns up to 50% of the production and dominates cobalt's supply chain. Tesla, VW Group and other manufacturers have zero-tolerance policy for child labour, but they are supplied with cobalt obtained in these inhuman conditions. In fact, Tesla, among other companies, has been accused of aiding and abetting in the death of children.

Much like the claim of electric cars being clean, these cars run on dirty energy on blood batteries. This is not climate change solution; this is human right abuse. And it must not be permitted to fight against global warming at the expense of human lives.

This scenario is not likely to get better, as it is expected that the demand for cobalt will increase a 585% by 2050. Unless cleaner and fair technologies emerge.

For all these reasons, the electric car cannot be the final step in the climate change fight in terms of mobility solutions, but an intermediate step.

Solar vehicle

It is very similar to the EV, with the difference that the battery recharging is made through solar panels installed on the car instead of connecting to the electrical grid. Although, most vehicles with solar

technology are just standard EVs with solar panels to increase their range.

Nowadays there is very little offer of pure solar vehicles, being the most known ones the Aptera and the Lightyear One.

The Aptera is a two-seater three-wheeler vehicle that claims to have up to 1000 km of range on a single charge and a top speed of more than 160 km/h. Its design is focused in reducing the aerodynamic friction losses, with its teardrop inspired shape, and as a result has a drag coefficient of just 0,19.

The Lightyear One is a photovoltaic car with a WLTP range of 725 km. The manufacturers assure that each hour the car is charged with solar energy 12 km are added to its range.

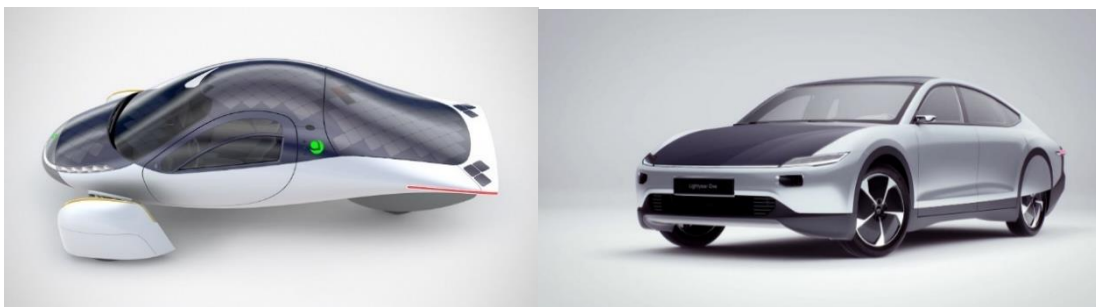


Fig. 50: Solar cars. Left: Aptera. Right: Lightyear One.

EVs fitted with solar panels have an advantage and a disadvantage in front of standard EVs. In one hand, the solar panels allow to travel further before needing to plug in to recharge, because the vehicle can recharge while driving or while being stationary outside under the shiny sky. There are cases in which the conventional recharging could not be required if the balance between the solar energy absorbed and the energy used is positive, such as the case of the Aptera. On the other hand, when manufacturing solar panels, some toxic and hazardous materials are used and those contribute to pollution.

And not to mention that as the EVs, the battery issue occurs with solar vehicles as well. And it has not to be forgotten that everything that involves the supply of rare materials from other countries may be problematic when geopolitical conflicts arise.

Hydrogen fuel cell vehicle

Here is what for most people is considered the next step to follow after EVs in the sustainability path. The main advantage of hydrogen fuel cell vehicles is that they have non-polluting tailpipe emissions, because these vehicles just emit H₂O vapor emissions.

The main counterpart of hydrogen fuel cell vehicles is that nowadays hydrogen fuel is obtained from a process that uses non-renewable natural gas and creates huge amounts of CO₂ emissions. As the other technologies, hydrogen fuel cell vehicles would only be 100% carbon emission-free if the hydrogen was produced from pure renewable resources.



Fig. 51: Hydrogen fuel cell vehicles. Left: BMW iX5 Hydrogen. Right: Pininfarina H2 Speed.

9.2. Advantages and disadvantages of compressed air

9.2.1. Advantages

An air powered car just exhausts air, clean breathable air, so it does not pollute. This means cleaner cities, better air quality, minor risk of respiratory diseases and less premature deaths due to contamination.

A compressed air vehicle powered by a Di Pietro motor is quieter than internal combustion engine cars. It is known that vehicle traffic is the main cause of acoustic contamination and its concerning effects on people's physical and mental health. Less noise will reduce the harmful effects on people's sleep, memory, attention, conduct and even pregnancy, among many others.

Unlike petrol or hydrogen vehicles, air is literally everywhere, so there is no need to process or prepare the "fuel". And do not forget that it is free. To refill a tank there just has to be paid the electricity used for the compressor to compress the air into the tank.

Air is intrinsically safe for use in hazardous areas or zones which must have a clean and hygienic environment because it is non-flammable and non-polluting. This makes air powered vehicles ideal for the pharmaceutical and chemical industry, dangerous explosive work atmospheres, areas with strong magnetic fields, hospitals and nursing homes, radio quiet zones and a long etcetera.

Compressed air bottles can be refilled up to 10000 times and they don't lose efficiency while aging. Furthermore, when their useful life comes to an end, these bottles can be recycled, having a minimal and almost insignificant environmental impact. This is especially important if it is compared to electric

vehicle, which their massive batteries are in most cases difficult to be recycled or directly non-recyclable.

Another growing problem with petrol or the rare metals used for the electric vehicle's batteries is that cause geopolitical conflicts for obtaining the control of these limited resources. This issue is impossible to happen with compressed air because, as said before, air is everywhere and within everyone's reach.

Electric and hydrogen cars need a huge charging infrastructure to support them, either home chargers or street chargers. The charging infrastructure for electric cars has grown considerably in the past years, although it is not big enough. But in the case of hydrogen cars, the hydrogen refuelling stations are non-existent or insignificant. Compressed air vehicles do not have this problem, as many petrol stations have air compressors to inflate the tires, and also can refill the compressed air tanks. Moreover, users could have a portable air compressor at home for night air refilling. So CAVs do not need the implementation of a new infrastructure of air refilling points.

Air powered vehicles require very little maintenance, and for so its related costs are very low, especially when compared with the costs of the electric or internal combustion engine counterparts. Also, the refilling costs are significantly lower than with current fuels.

The manufacturing costs of a compressed air vehicle are lower than those referred to the production of a fuel powered vehicle with similar performance characteristics. This is due to the fact that there is no need to manufacture the spark plugs, fuel pumps and other components only required in internal combustion engines.

The Compressed Air Energy Storage systems (CAES) are the least limited energy storage systems nowadays, as it can be seen in the following section "Energy Stored on Invested".

9.2.1.1. Energy Stored on Invested

Energy Stored on Invested (ESOI) is a metric which first appeared in a study made by Charles J. Barnhart and Sally M. Benson in 2013 for comparing the energy performance of storage technologies. In order to evaluate the different types of storage technologies, this metric does not just take into account the efficiency. Instead, it uses a combination of attributes which affect the energy cost of those storage technologies. ESOI allows to develop paths to energetic and material cost reduction.

In the study previously mentioned the energy storage technologies analysed with the ESOI metric were lithium ion (Li-ion), sodium sulphur (NaS) and lead-acid (PbA) batteries; vanadium redox (VRB) and zinc-bromine (ZnBr) flow batteries; and geologic pumped hydroelectric storage (PHS) and compressed air energy storage (CAES).

In the figure 52 is shown a quantification of the energy and material resource requirements for these energy storage technologies. It can be appreciated that the CAES is the least limited energy storage technology by its energetic requirements, while PbA batteries is the most limited one. It is remarkable the big gap between the different batteries and flow batteries technologies and the CAES and PHS technologies. Thus, the ESOI analysis shows the importance of compressed air technology for compared to electric batteries.

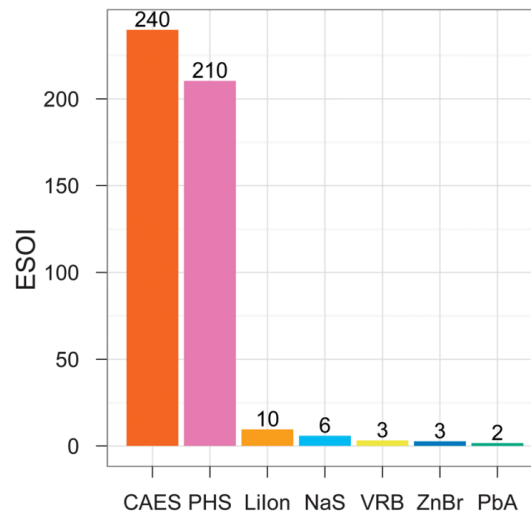


Fig. 52: ESOI for each type of energy storage technology.

9.2.2. Disadvantages

The main disadvantage of compressed air for a mobility application such this one is the weight of the air itself. The low energy density of air provokes that in order to have a decent autonomy range it has to be introduced in the tanks a considerable amount of air. In previous sections has been seen that in this study has been necessary to have close to 100 kg of air. In an urban vehicle application it may not be a problem at all, as the vehicle does not have to reach high speeds. However, it would be inconceivable to run a race car such as a Formula 1 car with compressed air.

Also, it may be an inconvenient the little knowledge people have about this alternative to power vehicles. At first people could be reticent about the idea having a compressed air car. Just to visualize this issue it has been created a graphic which compares around the world the interest of people in compressed air vehicles versus the interest in electric vehicles. To do that it has been used Google Trends, a tool of Google that measures the interest of people in a certain topic through the number of searches. The interest is measured with an index between a 0 to 100 range, where 100 is the most interest and 0 is the least interest.

The graphic can be seen in the figure 53 below, and it analyses the interest from January 1st of 2004 (when Google started to collect data of searches) to the present in the “automobiles and vehicles”

category.

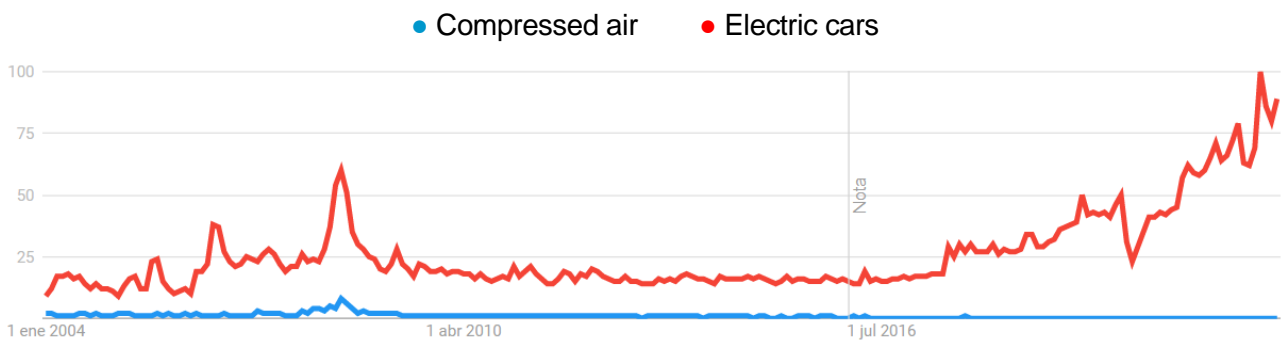


Fig. 53: Interest of compressed air vs electric cars from January of 2004 to June of 2022.

The note on the graphic at the 1st of July of 2016 only indicates a change in Google's data collection methods.

The interest analysis of the graphic is between compressed air and electric cars, not between compressed air cars and electric cars. This is because there were not enough data of searches about compressed air vehicles, so the interest in CAVs is in fact lower than the shown in the blue line.

Also, it has to be notice that air powered vehicles are likely to be not as sturdy as standard vehicles. This involves more danger for compressed air vehicles which share the same roads with bigger, heavier and more robust vehicles such as trucks or buses. For this reason, this vehicle has been intended to be used only in urban environments, where most streets have an upper speed limit of 30 km/h.

9.3. Environmental impact of the SG9C

As seen throughout these papers, one of the main purposes of the SG9C is to have the lowest environmental impact possible. For this reason, following next are listed the most important points referred to the environmental impact.

9.3.1. Emissions

The compressed air vehicle's main environmental advantage is that the only gas it exhausts is breathable air. Thus, if CAVs represent a significant percentage of the vehicle fleet of cities, this would imply a reduction of pollutant emissions, as fewer contaminant cars would be moving inside urbanized areas.

9.3.2. The air tanks

As seen in previous chapters, the air tanks have over 20 years of service life. To put it in context, on average a standard car has a 12-year lifespan, and EV's batteries have a useful life between 10 to 20

years. This means that the air tanks last on average nearly twice as a car and, in the best-case scenario, the same as the battery of an electric car.

The main difference is that the air tanks are not made of hard to recycle rare materials. At the end of their useful life, these air bottles are recyclable, in an easier way than the EV's batteries.

9.3.3. The chassis and body

As the chassis is made of aluminium, it can be easily recycled with the existing aluminium recycling methods. During the aluminium recycling process, it is only emitted the 5% of the carbon dioxide emitted during the aluminium obtaining process from raw material.

As seen previously, the body of the vehicle can be made in two different ways. The first one would be the body made of composite materials and the second one would be a polycarbonate body.

Although both composite materials and polycarbonates may be difficult to recycle and the processes in most cases are expensive, new recycling methods are emerging, and each year more companies are putting more resources and efforts into recycling these types of materials. For so, composite and polycarbonate materials are thought to be easier and cheaper to recycle in the coming years.

10. Economic study

10.1. Economic comparative

10.1.1. Refilling costs

To compare the cost per 100 km of the three different technologies it has been considered vehicles as similar as possible to the SG9C. For so, the fuel vehicle used is the Smart Fortwo Coupe W453 with 45 kW, the EV is logically the Citroën Ami and the CAV is one of Angelo Di Pietro's prototypes. In the following table is shown the data and the resulting cost per 100 km.

	Smart Fortwo Coupe W453 with 45 kW	Citroën Ami	SG9C
Technology	Fuel	Electric	Compressed air
Consumption	4,5 L/100 km	5,5 kWh/70 km	10,37 kWh/50 km
Resource price	2,05 €/L	0,24 €/kWh	0,24 €/kWh
$\frac{\text{€}}{100 \text{ km}}$	9,22	1,89	4,98

Table 13: Refilling costs comparative.

Note that for the SG9C has been imposed the worst-case scenario, in which the available 10,37 kWh of energy stored in the air tanks are used in the minimum autonomy range of only 50 km. In case of having a 100 km range, the cost would be half 2,49 € per each 100 km.

10.1.2. Overall cost

The SG9C is expected to have a lower price than its competitors, because the costs have been reduced in multiple ways. Firstly, the engine would be cheap to produce. At the beginning each Di Pietro engine is thought to cost \$5000 (which yet is less than most petrol engines), but once it is in chain production, it is thought to cost only \$500 due to its very few components. Secondly, the vehicle does not need huge expensive electric batteries, just the more affordable air tanks. Moreover, in the market research it has been seen that the Citroën Ami is sold from 7600€, which uses electric batteries that are more expensive to manufacture than compressed air tanks. Finally, the symmetrical design is intended to reduce the overall cost of the manufacturing, so at the very end of the process with the information known the vehicle should be sold under 7500€.

10.2. Project implementation budget

The duration of the project has been of 5 months, which comprehend from the 1st of February to the 26th of June. This time period has consisted of 21 weeks, or what is the same, 146 days, 104 of them weekdays and the remaining 42 being weekend days.

In the itemized cost list when the time duration of the cost is expressed in months means that the specified item has had a cost every day. Otherwise, when the cost is not expressed in months means that the item just has cost during the defined number of hours, days or weeks.

To estimate the cost of the project has been used the author's real bills of the items listed below in the table 14. To calculate the staff cost has been considered the average industrial engineer salary in Spain.

Item	Unitary cost	Duration	Item cost
Staff cost			
- Industrial Engineer	13,4 €/hour	840 hours	11256 €
Equipment cost			
- Computer	40 €/month	5 months	200 €
- Printer	5 €/month	5 months	25 €
Expandable material cost (Paper, ink, office utensils...)	20 €/month	5 months	100 €
Displacement costs			
- Meals	30 €/day	5 months	150 €
- Transportation	44 €/month	5 months	220 €
Other costs			
- Light	94 €/month	5 months	470 €
- Water	51 €/month	5 months	255 €
- Communications (Telephone line, Wi-Fi, 4G...)	203 €/month	5 months	1015 €
TOTAL (before taxes)			13691 €

Table 14: Itemized cost list of the project.

Conclusions

Due to the climate change and all the environmental issues that go with it the compressed air car appears as a truly eco-friendly mobility alternative. But this is not a utopic solution. Throughout this study has been demonstrated that a compressed air urban vehicle equipped with the powertrain designed and powered by the Di Pietro engine is a feasible option to move people around cities.

As seen in these papers, electric vehicles are a step forward from fuel vehicles. However, EVs cannot be the final step in the sustainable mobility field, but an intermediate step. It is clear that there are greener alternatives, as it has been shown with the compressed air for urban mobility applications. Day by day, oil is becoming a scarcer resource, and for so it should be reserved for those applications which do not have any other alternative nowadays, such as large-scale air or maritime transport. Using fuel for small land vehicles is the waste of a very limited resource.

It has been found that a vehicle like this one has the potential to be affordable enough to be competitive with its petrol and electric counterparts in their market segment.

The future work that is intended to come after these papers comprehend all the necessary steps to materialize the SG9C. The most important future work is listed below:

- To design the tubular frame chassis and the bodywork.
- To perform a structural analysis of the tubular frame chassis and the bodywork.
- To design the internal pneumatic cabling.
- To study the viability of installing an air heater between the air tank and the Di Pietro motor in order to double the autonomy range.
- To evaluate the convenience of the replaceable tank refilling method.
- Selecting a suitable air compressor for home refilling.
- To study the limitations of the SG9C with a physical prototype.
- To do an exhaustive economic study of the whole manufacturing process of the vehicle.
- Designing a business plan for the vehicle manufacturing.
- Licensing the Di Pietro engine in order to be able to manufacture vehicles with it.

Acknowledgements

The author of the present project would like to thank all the people following next. The author wants to thank:

Carlos Sierra Garriga, for his guidance and support, and for giving the author absolute freedom to do this project. Also, for introducing him to the compressed-air vehicle and planting the curiosity seed to research more about it.

Ali Osman Konuray, for helping the author to solve some thermodynamics doubts and giving useful advice.

Alexandre Presas, for giving guidance in the matter of fluid mechanics and helping the author to solve some doubts about it.

Daniel Montesinos, for providing the author with useful tools and knowledge in his Automotive Project subject.

Angelo Di Pietro, for having invented the revolutionary Di Pietro engine and for providing the author with useful data about it.

And now, putting aside this impersonal tone, I would like to thank:

I would like to thank my family, for all the incessantly infinite support I have received from them.

I would like to thank my brother, who no matter when manages to make me smile and laugh. He has always been in the best moments of my life and I couldn't have a better brother than him.

I would like to thank my mother, for taking care of innumerable things, helping me whenever I needed and for being the guide I followed in the hardest moments.

And finally, I would like to thank my father, who always encouraged me to follow my crazy ideas and with whom I have shared 20 beautiful years. Thanks to him and my mother, today I am who I am, and I could never thank them enough for everything they have done.

Bibliography

Bibliographic references

- [1] MEHRDAD EHSANI, YIMIN GAO and EMADI, Ali, 2010b. *Modern electric, hybrid electric, and fuel cell vehicles : fundamentals, theory, and design*. Boca Raton: Crc Press. ISBN 9781420053982.
- [2] Environmentally Friendly, Engine, Invention | Melbourne, 2020. *Engineair.com.au*. Online. [Accessed 21 February 2022]. Available from: <https://www.engineair.com.au/>
- [3] GEORGE, Alexander, 2012. Air-Powered Motorcycle Runs on Scuba Tank, Rotary Engine. *Wired*. Online. 6 November 2012. [Accessed 13 April 2022]. Available from: <https://www.wired.com/2012/11/air-motorcycle>
- [4] The Angell Project, 2014. *Issuu*. Online. [Accessed 8 April 2022]. Available from: https://issuu.com/martylaurita/docs/thesis_book_pages
- [5] Behance, 2022. *Behance.net*. Online. [Accessed 13 April 2022]. Available from: <https://www.behance.net/gallery/8865165/Airgo>
- [6] Kangaroo motorcycle – www.bartvandriessche.nl, 2022. *Bartvandriessche.nl*. Online. [Accessed 13 April 2022]. Available from: https://bartvandriessche.nl/portfolio_page/kangaroo_motorcycle/
- [7] ZWIERZCHOWSKI, Jaroslaw, 2017. Design type air engine Di Pietro. DANČOVÁ, P. (ed.), *EPJ Web of Conferences*. Online. 2017. Vol. 143, p. 02149. [Accessed 13 April 2022]. DOI 10.1051/epjconf/201714302149.
- [8] JAROSŁAW ZWIERZCHOWSKI, 2017. Design type air engine Di Pietro. *ResearchGate*. Online. 2017. [Accessed 13 April 2022]. Available from: https://www.researchgate.net/publication/316884692_Design_type_air_engine_Di_Pietro

- [9] [HTTPS://NEWATLAS.COM/AUTHOR/MIKE-HANLON](https://newatlas.com/author/mike-hanlon), 2004. Significant new rotary engine design runs on compressed air. *New Atlas*. Online. 15 September 2004. [Accessed 14 April 2022]. Available from: <https://newatlas.com/go/3185/>
- [10] An engine with no polluting emissions - WWF-Australia, 2013. *Wwf.org.au*. Online. [Accessed 14 April 2022]. Available from: <https://www.wwf.org.au/news/blogs/zero-emissions-engine-is-a-perfect-10>
- [11] Il Motore ad Aria è Realtà. Intervista con Angelo Di Pietro della Engineair e la sua straordinaria invenzione. Rivoluzionare il trasporto con un motore ad aria ora è possibile, 2015. *Genitronsviluppo.com*. Online. [Accessed 19 April 2022]. Available from: <http://www.genitronsviluppo.com/2008/06/10/il-motore-ad-aria-e-realta-intervista-con-angelo-di-pietro-della-engineair-e-la-sua-straordinaria-invenzione-rivoluzionare-il-trasporto-con-un-motore-ad-aria-ora-e-possibile/>
- [12] Error, [no date]. *www.miteco.gob.es*. Online. [Accessed 23 April 2022]. Available from: https://www.miteco.gob.es/images/es/17a.%20Ciutat%2030%20Argumentos%20b%C3%A1sicos_tcm30-169494.pdf
- [13] ARCHINAUTA, 2007. RENDIMENTO MOTORE ARIA COMPRESSA. *Blogspot.com*. Online. 8 August 2007. [Accessed 23 April 2022]. Available from: <http://archinauti.blogspot.com/2007/08/rendimento-motore-aria-compressa.html>
- [14] PAVLOVIC, Ana and CRISTIANO FRAGASSA, 2015. General considerations on regulations and safety requirements for quadricycles. *ResearchGate*. Online. December 2015. [Accessed 3 May 2022]. Available from: https://www.researchgate.net/publication/287521319_General_considerations_on_regulations_and_safety_requirements_for_quadricycles
- [15] BURROWS, Adrian, 2013. EU Regulation on the Approval of L-Category Vehicles.
- [16] WIKIPEDIA CONTRIBUTORS, 2022. Quadricycle (EU vehicle classification). *Wikipedia*. Online. 9 November 2021. [Accessed 4 May 2022]. Available from: [https://en.wikipedia.org/wiki/Quadricycle_\(EU_vehicle_classification\)#Categories](https://en.wikipedia.org/wiki/Quadricycle_(EU_vehicle_classification)#Categories)

- [17] WIKIPEDIA CONTRIBUTORS, 2022. Compressed air car. *Wikipedia*. Online. 26 April 2022. [Accessed 4 May 2022]. Available from: https://en.wikipedia.org/wiki/Compressed_air_car
- [18] WIKIPEDIA CONTRIBUTORS, 2022. Air pollution. *Wikipedia*. Online. 3 May 2022. [Accessed 4 May 2022]. Available from: https://en.wikipedia.org/wiki/Air_pollution
- [19] WIKIPEDIA CONTRIBUTORS, 2022. Vehicle category. *Wikipedia*. Online. 14 March 2022. [Accessed 6 May 2022]. Available from: https://en.wikipedia.org/wiki/Vehicle_category
- [20] SHERMAN, Don, 2015. How a Car is Made: Every Step from Invention to Launch. *Car and Driver*. Online. 18 November 2015. [Accessed 6 May 2022]. Available from: <https://www.caranddriver.com/news/a15350381/how-a-car-is-made-every-step-from-invention-to-launch/>
- [21] Car Design: From the Drawing Board to Production - Inspirationfeed, 2012. *Inspirationfeed*. Online. [Accessed 6 May 2022]. Available from: <https://inspirationfeed.com/car-design-from-the-drawing-board-to-production/>
- [22] MDI | Compressed Air Engine | Luxembourg, 2015. *MDI Group*. Online. [Accessed 7 May 2022]. Available from: <https://www.mdi.lu/>
- [23] BARNHART, Charles J. and BENSON, Sally M., 2013. On the importance of reducing the energetic and material demands of electrical energy storage. *Energy & Environmental Science*. 2013. Vol. 6, no. 4, p. 1083. DOI 10.1039/c3ee24040a.
- [24] REGLAMENTO (UE) N o 168/2013 DEL PARLAMENTO EUROPEO Y DEL CONSEJO, [no date]. Online. [Accessed 12 May 2022]. Available from: <https://www.boe.es/doue/2013/060/L00052-00128.pdf>
- [25] Type IV CNG Cylinder, 2017. *Timetechnoplast.com*. Online. [Accessed 13 May 2022]. Available from: <https://www.timetechnoplast.com/business-division/composite-cylinder/type-iv-cng-cylinder/>

- [26] Emission Test Cycles: ECE 15 + EUDC / NEDC, 2013. *Dieselnet.com*. Online. [Accessed 21 May 2022]. Available from: https://dieselnet.com/standards/cycles/ece_eudc.php
- [27] 2015. *Www.mdi.lu*. Online. [Accessed 24 May 2022]. Available from: <https://www.mdi.lu/airpod-technical-sheet>
- [28] AirPod standard specifiche - Air Mobility, 2019. Air Mobility. Online. [Accessed 24 May 2022]. Available from: <https://www.airmobility.it/airpod-standard-specifiche/>
- [29] airpod standard 2.0 - Air Mobility, 2019. Air Mobility. Online. [Accessed 24 May 2022]. Available from: <https://www.airmobility.it/airpod-standard-20/>
- [30] Airpod technical sheet | MDI Group, 2015. MDI Group. Online. [Accessed 24 May 2022]. Available from: <https://www.mdi.lu/airpod-technical-sheet>
- [31] INNOVATIONS — AIR FUTURE, 2014. Air Future. Air Future. Online. 2014. [Accessed 24 May 2022]. Available from: <https://www.airfuture.co.nz/innovations>
- [32] MDI, 2021. MDI Corporate Brochure. MDI Corporate Brochure. Online. 13 March 2021. [Accessed 24 May 2022]. Available from: <https://static1.squarespace.com/static/5b27166a89c172b2f5cd1d33/t/601a529274877352c1c46e10/1612337838385/MDI+Corporate+Brochure+-+A5+Booklet.pdf>
- [33] SURAM SINGH VERMA, 2008. Air Powered Vehicles. ResearchGate. Online. 13 October 2008. [Accessed 25 May 2022]. Available from: https://www.researchgate.net/publication/228403289_Air_Powered_Vehicles
- [34] 2022. *Enggcyclopedia.com*. Online. [Accessed 4 June 2022]. Available from: <https://www.enggcyclopedia.com/2011/09/air-compressibility-factor-table/>
- [35] GOOGLE TRENDS, 2015. Google Trends. *Google Trends*. Online. 2015. [Accessed 19 June 2022]. Available from:

<https://trends.google.es/trends/explore?cat=47&date=all&q=Compressed%20air,Electric%20car>

- [36] Termodinàmica : taules i gràfiques de propietats termodinàmiques, 2008. Barcelona: ETSEIB. CPDA.